Rare K and B decays in the littlest Higgs model without T-parity

Andrzej J. Buras,[a] **Anton Poschenrieder,**[a] **Selma Uhlig**[a] **and William A. Bardeen**[b]

[a]*Physik Department, Technische Universität München*
D-85748 Garching, Germany
[b]*Theoretical Physics Department, Fermilab*
Batavia, IL 60510, U.S.A.
E-mail: `andrzej.buras@ph.tum.de`, `anton.poschenrieder@ph.tum.de`,
`selma.uhlig@ph.tum.de`, `bardeen@fnal.gov`

ABSTRACT: We analyze rare K and B decays in the Littlest Higgs (LH) model *without* T-parity. We find that the final result for the Z^0-penguin contribution contains a divergence that is generated by the one-loop radiative corrections to the currents corresponding to the dynamically broken generators. Including an estimate of these logarithmically enhanced terms, we calculate the branching ratios for the decays $K^+ \to \pi^+ \nu\bar\nu$, $K_{\rm L} \to \pi^0 \nu\bar\nu$, $B_{s,d} \to \mu^+\mu^-$ and $B \to X_{s,d}\nu\bar\nu$. We find that for the high energy scale $f = \mathcal{O}(2-3)$TeV, as required by the electroweak precision studies, the enhancement of all branching ratios amounts to at most 15% over the SM values. On the technical side we identify a number of errors in the existing Feynman rules in the LH model without T-parity that could have some impact on other analyses present in the literature. Calculating penguin and box diagrams in the unitary gauge, we find divergences in both contributions that are cancelled in the sum except for the divergence mentioned above.

KEYWORDS: Rare Decays, B-Physics, Beyond Standard Model.

Contents

1. Introduction

The Little Higgs models [1]-[5] offer an attractive and a rather simple solution to the gauge hierarchy problem. In these models the electroweak Higgs boson is regarded as a pseudo-Goldstone boson of a certain global symmetry that is broken spontaneously at a scale $f \sim \mathcal{O}\,(1\,\text{TeV})$, much higher than the vacuum expectation value v of the standard Higgs doublet. The Higgs field remains then light, being protected by the approximate global symmetry from acquiring quadratically divergent contributions to its mass at the one-loop

level. On the diagrammatic level the new heavy particles present in these models cancel, analogously to supersymmetric particles, the quadratic divergencies in question. Reviews on the Little Higgs models can be found in [6].

One of the simplest models of this type is the "Littlest Higgs" model [4] (LH) in which, in addition to the Standard Model (SM) particles, new charged heavy vector bosons ($W_H^\pm$), a neutral heavy vector boson (Z_H^0), a heavy photon (A_H^0), a heavy top quark (T) and charged and neutral heavy Higgs scalars are present. Among the scalars only the single charged scalar ($\Phi^\pm$) is important in principle for rare decays. The details of this model including the Feynman rules have been worked out in [7] and the constraints from various processes, in particular from electroweak precision observables and direct new particles searches, have been extensively discussed in [7]-[13]. It has been found that except for the heavy photon A_H^0, that could still be as "light" as 500 GeV, the masses of the remaining particles are constrained to be significantly larger than 1 TeV.

Much less is known about the flavour changing neutral current (FCNC) processes in the LH model. As these processes played an essential role in the construction of the SM and in the tests of its extensions, it is important to check whether the LH model is consistent with the existing data on FCNC processes and whether the deviations from the SM expectations predicted in this model are sufficiently large so that they could be detected in present and future experiments.

In [14] we have calculated the $K^0 - \bar{K}^0$, $B_{d,s}^0 - \bar{B}_{d,s}^0$ mixing mass differences ΔM_K, $\Delta M_{d,s}$ and the CP-violating parameter ε_K in the LH model. We have found that even for f/v as low as 5, the enhancement of ΔM_d amounts to at most 20% for the Yukawa parameter $x_L \leq 0.8$. Similar comments apply to ΔM_s and ε_K. The correction to ΔM_K is negligible. These results have been confirmed in [15]. Larger effects could be present in $D^0 - \bar{D}^0$ mixing [16], where in contrast to processes involving external down quarks, FCNC transitions are already present at the tree level. But as analyzed in [17] these effects are small.

On the other hand we have pointed out in [14, 18] that for $0.80 \leq x_L \leq 0.95$ and $f/v \leq 10$, which is still allowed by the electroweak precision studies, the non-decoupling effects of the heavy T can significantly suppress the CKM element $|V_{td}|$ and the angle γ in the unitarity triangle and simultaneously enhance ΔM_s. The recent data from CDF and DØ collaborations [19, 20] disfavour this possibility, although in view of large non-perturbative uncertainties in the evaluation of ΔM_s nothing conclusive can be said at present [21, 22].

Concerning FCNC decay processes only $B \to X_s \gamma$ and $K_L \to \pi^0 \nu \bar{\nu}$ have been considered so far in the literature. While in [23] the LH corrections to the the decay $B \to X_s \gamma$ have been found to be small, a large enhancement of the branching ratio for $K_L \to \pi^0 \nu \bar{\nu}$ relative to the SM expectations has been found in [24].

In the present paper we extend our study of FCNC processes in the LH model to the rare decays $K^+ \to \pi^+ \nu \bar{\nu}$, $K_L \to \pi^0 \nu \bar{\nu}$, $B_{s,d} \to \mu^+ \mu^-$ and $B \to X_{s,d} \nu \bar{\nu}$. We also briefly discuss the decay $B \to X_s \gamma$.

The analysis of the rare decays in question turned out to be much more involved than the one of particle–antiparticle mixing due to the presence of many more diagrams, in particular the Z^0, Z_H^0 and A_H^0 penguins that were absent in our previous study. In

order to reduce the number of contributing diagrams we have performed all calculations in the unitary gauge for the $W_L^\pm$ and $W_H^\pm$ propagators which has the nice virtue that only exchanges of physical particles have to be considered.

Already in [14, 18] we have found that the box diagrams contributing to particle-antiparticle mixing were divergent in the unitary gauge but these divergences cancelled each other after the unitarity of the CKM matrix in the SM has been used and the contribution of the heavy T included at $\mathcal{O}(v^2/f^2)$. Simply, the GIM mechanism [25] was sufficiently effective to remove these divergences. In the case of rare decays, to which also penguin diagrams contribute, the cancellation of divergences, even in the SM, is more involved due to a different structure of the diagrams. It turns out that the contributions of box diagrams to decay amplitudes remain divergent even after the GIM mechanism has been used. However the full contribution of penguin diagrams is also divergent and in the SM this divergence cancels the one from the box diagrams.

On the other hand in our analysis of the complete set of contributions to the weak decay amplitudes in the LH model we find a remaining divergence in our unitary gauge calculation. While all divergent contributions from the box diagrams are exactly cancelled by gauge related divergences of the vertex contributions as in the SM, there is a remaining divergence generated by the radiative corrections to the quark vertex. The origin of this divergence can be traced to the structure of charge renormalization for the currents associated with the dynamically broken generators. For linearly realized symmetries, current conservation implies that the charges are not renormalized by radiative corrections. However, conserved currents associated with dynamically broken charges are not protected from renormalization and the charge vertex can be modified by the radiative corrections. The currents remain conserved because there is a corresponding modification of the Goldstone boson contribution to the current matrix element. In the nonlinear sigma model used to describe the little Higgs theory, these contributions can be divergent and depend on the UV completion of the theory. In a linear sigma model, the UV cutoff would be identified with symmetry breaking within the meson multiplet and related to the masses of the heavy partners to the Goldstone bosons. A more general UV completion may even include charge renormalization at tree level.

This mechanism is analogous to the dynamics associated with renormalization of axial-vector charge, G_A, in the constituent quark model. In particular, Peris [26] has shown that the axial charge of the constituent quark is suppressed by the one-loop radiative corrections in agreement with the quark model description of the axial charge of the physical baryons. The divergent contributions to the weak decay amplitudes will be discussed in more detail in Section 5.

In the process of our analysis we found several errors in certain Feynman rules for the v^2/f^2 corrections to the $Z^0 \bar{f} f$ vertices and in the vertices involving the heavy T that were given in [7]. Without correcting these rules the final result would contain many more divergences and parametric dependencies that should be absent.

We are not the first to consider the decay $K_L \to \pi^0 \nu\bar{\nu}$ within the LH model. In [24] this decay has been analyzed with the result that its branching ratio could be enhanced by a factor of two or more by LH contributions relative to the SM expectations [27]. This

would be a very nice result as an enhancement of this size in a theoretically clean decay $K_{\mathrm{L}} \to \pi^0 \nu\bar{\nu}$ could clearly be distinguished from the SM in future experiments.

Unfortunately our analysis of $K_{\mathrm{L}} \to \pi^0 \nu\bar{\nu}$ presented here does not confirm the findings of [24]. This possibly can be traced back to the fact that these authors used the Feynman rules of [7] that according to our analysis cannot give correct results for rare decay branching ratios in question. There is also the following qualitative difference between the final results presented in [24] and ours. It is related to the additional weak mixing angle s', present in the LH model, that is analogous to $\sin\theta_w$ in the SM. The short distance function X relevant for FCNC processes with $\nu\bar{\nu}$ in the final state cannot depend on $\sin\theta_w$ and s' due to current conservation. Our results for X and the function Y, relevant for the FCNC processes with l^+l^- in the final state, are indeed independent of $\sin\theta_w$ and s', while the numerical results presented in [24] show a clear s' dependence.

The main goal of our paper is the calculation of the LH contributions to the short distance functions X and Y [28, 29]. This will allow us to compute the impact of these contributions on various rare K and B decay branching ratios, which enter universally all decays in models with minimal flavour violation [30] such as the LH model considered here. Our main findings for $K^+ \to \pi^+ \nu\bar{\nu}$, $K_{\mathrm{L}} \to \pi^0 \nu\bar{\nu}$, $B_s \to \mu^+\mu^-$ in the limit $x_L \approx 1$ have been summarized in [18]. In this limit ΔM_s can be significantly enhanced with respect to the SM, although this limit seems to be disfavoured by the recent CDF and DØ data. Here we present the details of these investigations in the full space of the parameters involved, that requires the inclusion of many more diagrams. We also extend our analysis to other rare decays and to the $B \to X_s\gamma$ decay.

Our paper is organized as follows. In Section 2 we recall briefly those elements of the LH model that are necessary for the discussion of our calculation. In particular we give the $U(1)$ charges for quarks and leptons and present the list of the relevant Feynman rules that at various places differ from those found in [7].

In Section 3 we discuss the functions X and Y within the SM, presenting for the first time the expressions for the Z^0 penguin function C and the relevant box functions $B^{\nu\bar{\nu}}$ and $B^{\mu\bar{\mu}}$ in the unitary gauge. All these functions are divergent but inserting them in the expressions for X and Y one recovers the known finite results. The result for C in the unitary gauge will be particularly relevant for our LH calculation.

Section 4 is devoted to the calculation of X and Y within the LH model. We group the diagrams in six classes. We present analytic results for each class and for the full correction to the functions X and Y. In three of these classes the divergences in diagrams belonging to a given class cancel each other. In the remaining classes the divergences with a simple structure remain. In Section 5 we discuss in more detail the origin of the leftover divergences that could be of interest for other little Higgs models. We also give an estimate of these logarithmic enhanced terms, which turn out to be small.

In Section 6 we present the numerical results for various branching ratios. Thanks to compendia in [31, 34, 35], that give various branching ratios in terms of the functions X and Y we do not have to list once again all these formulae so that this section can be kept brief in spite of many decays involved.

In Section 7 we first briefly discuss the $B \to X_s\gamma$ decay confirming basically the result

of [23]. A brief summary of our paper is given in Section 8. Some technicalities are relegated to the appendices.

2. Aspects of the Littlest Higgs Model

2.1 Gauge Boson Sector

Let us first recall certain aspects of the LH model that are relevant for our work. The full exposition can be found in the original paper [4] and in [7]. We will follow as far as possible the notations of [7].

The global symmetry in the LH model is a $SU(5)$ with a locally gauged subgroup

$$G_1 \otimes G_2 = [SU(2)_1 \otimes U(1)_1] \otimes [SU(2)_2 \otimes U(1)_2] . \tag{2.1}$$

In the process of the spontaneous breakdown of the global $SU(5)$ at a scale $f \sim 1$ TeV to a global $SO(5)$, the gauge group $G_1 \otimes G_2$ is broken down to the electroweak SM gauge group $SU(2)_L \otimes U(1)_Y$. The resulting mass eigenstates in the gauge boson sector are

$$W = s\,W_1 + c\,W_2, \qquad\qquad B = s'B_1 + c'B_2, \tag{2.2}$$
$$W' = -c\,W_1 + s\,W_2, \qquad\qquad B' = -c'B_1 + s'B_2. \tag{2.3}$$

Here W_1 and W_2 represent symbolically the three gauge bosons of $SU(2)_1$ and $SU(2)_2$, respectively. B_1 and B_2 are the corresponding gauge bosons of $U(1)_1$ and $U(1)_2$.

Note that $W = W_1$, $W' = W_2$, $B = B_1$, $B' = B_2$ for $s = 1$ and $s' = 1$ and not for $s = 0$ and $s' = 0$. Thus in fact s, s', c and c' are the sines and cosines of the mixing angles plus 90 degrees and not of the mixing angles as usually done in other cases in the literature. The replacements $s \to c$ and $c \to s$ would be certainly a better choice. However, in order not to mix up the comparison of Feynman rules presented here with the ones of [7] we will use the conventions of these authors, remembering that the mixing between various groups is absent for $s = 1$ and $s' = 1$.

We have

$$s = \frac{g_2}{\sqrt{g_1^2 + g_2^2}}, \qquad c = \frac{g_1}{\sqrt{g_1^2 + g_2^2}}, \tag{2.4}$$

$$s' = \frac{g_2'}{\sqrt{g_1'^2 + g_2'^2}}, \qquad c' = \frac{g_1'}{\sqrt{g_1'^2 + g_2'^2}}, \tag{2.5}$$

where $g_{1,2}$ are the $SU(2)_{1,2}$ coupling constants and $g_{1,2}'$ the ones of the $U(1)_{1,2}$.

The W' and B' gauge bosons receive the heavy masses

$$m_{W'} = \frac{f}{2}\sqrt{g_1^2 + g_2^2} = \frac{g}{2sc}f, \qquad m_{B'} = \frac{f}{2\sqrt{5}}\sqrt{g_1'^2 + g_2'^2} = \frac{g'}{2\sqrt{5}s'c'}f, \tag{2.6}$$

while the fields W and B remain massless at this stage and can be identified as the SM gauge bosons with the couplings g and g' given by

$$g = g_1 s = g_2 c, \qquad g' = g_1' s' = g_2' c'. \tag{2.7}$$

In the second step of the gauge symmetry breaking the SM group is broken down to $U(1)_Q$. The details of this breakdown are presented in [7]. As our results differ at certain places from those given in this paper, we give below the most relevant formulae summarizing subsequently the differences.

The mass eigenstates of the gauge bosons can be obtained by diagonalizing

$$
\begin{aligned}
\mathcal{L}_{masses} = {}& W_\mu'^a W'^{a\mu} \left(\frac{m_{W'}^2}{2} - \frac{1}{8} g^2 v^2 \right) + (W_\mu^1 W^{1\mu} + W_\mu^2 W^{2\mu}) \left(\frac{1}{8} g^2 v^2 \left(1 + r \frac{v^2}{f^2} \right) \right) \\
& + W_\mu^3 W^{3\mu} \left(\frac{1}{8} g^2 v^2 \left(1 + r \frac{v^2}{f^2} \right) \right) + W_\mu^a W'^{a\mu} \left(-\frac{1}{4} g^2 v^2 \frac{(c^2 - s^2)}{2sc} \right) \\
& + B_\mu' B'^\mu \left(\frac{m_{B'}^2}{2} - \frac{1}{8} g'^2 v^2 \right) + B_\mu B^\mu \left(\frac{1}{8} g'^2 v^2 \left(1 + r \frac{v^2}{f^2} \right) \right) \\
& + B_\mu B'^\mu \left(-\frac{1}{4} g'^2 v^2 \frac{(c'^2 - s'^2)}{2s'c'} \right) + W_\mu^3 B^\mu \left(\frac{1}{4} gg' v^2 \left(1 + r \frac{v^2}{f^2} \right) \right) \\
& + W_\mu'^3 B'^\mu \left(-\frac{1}{8} gg' v^2 \left(\frac{cs'}{sc'} + \frac{sc'}{cs'} \right) \right) + W_\mu^3 B'^\mu \left(-\frac{1}{4} gg' v^2 \frac{(c'^2 - s'^2)}{2s'c'} \right) \\
& + W_\mu'^3 B^\mu \left(-\frac{1}{4} gg' v^2 \frac{(c^2 - s^2)}{2sc} \right),
\end{aligned}
\tag{2.8}
$$

with v denoting the vacuum expectation of the neutral components of the complex doublet. In our analysis we will set the vacuum expectation of the Higgs triplet v' to zero. For the parameter r in (2.8) we find $r = -1/6$ that agrees with (A30) in [7] but differs from [8], where $r = 1/2$ can be found. This difference has no direct impact on our calculation and as discussed in [8] can be absorbed through the redefinition of the parameters involved.

The final mass eigenstates of the charged gauge bosons are $W_L^\pm$ and $W_H^\pm$ where the indices L and H stand for "light" and "heavy". The mass eigenstates are

$$
W_L = W + \frac{v^2}{2f^2} sc(c^2 - s^2) W', \qquad W_H = W' - \frac{v^2}{2f^2} sc(c^2 - s^2) W,
\tag{2.9}
$$

and the corresponding masses read ($r = -1/6$)

$$
M_{W_L^\pm}^2 = m_w^2 \left(1 - \frac{v^2}{f^2} \left(-r + \frac{1}{4}(c^2 - s^2)^2 \right) \right)
\tag{2.10}
$$

$$
M_{W_H^\pm}^2 = m_w^2 \left(\frac{f^2}{s^2 c^2 v^2} - 1 \right).
\tag{2.11}
$$

The mass of the $W^\pm$ boson in the SM is given by $m_w \equiv gv/2$.

The neutral gauge boson mass eigenstates are A_L, Z_L, A_H and Z_H given by

$$
\begin{aligned}
A_L &= -s_w W^3 + c_w B, \\
Z_L &= c_w W^3 + s_w B + x_Z^{W'} \frac{v^2}{f^2} W'^3 + x_Z^{B'} \frac{v^2}{f^2} B', \\
A_H &= B' + x_H \frac{v^2}{f^2} W'^3 - x_Z^{B'} \frac{v^2}{f^2} (c_w W^3 + s_w B),
\end{aligned}
$$

$$Z_H = W'^3 - x_H \frac{v^2}{f^2} B' - x_Z^{W'} \frac{v^2}{f^2} (c_w W^3 + s_w B), \tag{2.12}$$

with

$$
\begin{aligned}
x_H &= \frac{5}{2} g g' \frac{scs'c'(c^2 s'^2 + s^2 c'^2)}{(5g^2 s'^2 c'^2 - g'^2 s^2 c^2)}, \\
x_Z^{W'} &= \frac{1}{2c_w} sc(c^2 - s^2), \\
x_Z^{B'} &= \frac{5}{2s_w} s'c'(c'^2 - s'^2).
\end{aligned}
\tag{2.13}
$$

Here

$$s_w = \frac{g'}{\sqrt{g^2 + g'^2}}, \qquad c_w = \frac{g}{\sqrt{g^2 + g'^2}}. \tag{2.14}$$

are the sine and the cosine of the Weinberg angle describing the weak mixing in the SM.

A_L and Z_L are the SM photon and Z^0 boson and A_H and Z_H the new heavy photon and heavy Z^0 boson, respectively. Their masses are given by ($r = -1/6$)

$$M_{A_L}^2 = 0, \tag{2.15}$$

$$M_{Z_L}^2 = m_z^2 \left(1 - \frac{v^2}{f^2} \left(-r + \frac{1}{4}(c^2 - s^2)^2 + \frac{5}{4}(c'^2 - s'^2)^2 \right) \right), \tag{2.16}$$

$$M_{A_H}^2 = m_z^2 s_w^2 \left(\frac{f^2}{5 s'^2 c'^2 v^2} - 1 \right), \tag{2.17}$$

$$M_{Z_H}^2 = m_w^2 \left(\frac{f^2}{s^2 c^2 v^2} - 1 \right), \tag{2.18}$$

where m_z is the SM Z^0 boson mass with $m_z \equiv gv/(2c_w)$.

It is evident from (2.10) and (2.16) that the tree level SM relation

$$\frac{m_w^2}{m_z^2} = c_w^2 \tag{2.19}$$

is not valid for the $W_L^\pm$ and Z_L^0 masses. To $\mathcal{O}(v^2/f^2)$ we have [7]

$$\frac{M_{W_L^\pm}^2}{M_{Z_L}^2} = c_w^2 \left(1 + \frac{v^2}{f^2} \frac{5}{4}(c'^2 - s'^2)^2 \right) \tag{2.20}$$

which manifests the breaking of the custodial $SU(2)$ in the LH model. Formula (2.20) will play an important role in our analysis.

From (2.10) and (2.11) we find

$$M_{W_H^\pm} = \frac{f}{v} \frac{M_{W_L^\pm}}{sc}, \tag{2.21}$$

which is valid to order v^2/f^2.

The formulae given above have been already presented in [7] but at a few places our results differ from the ones presented there. We would like to spell out these differences explicitly.

- In going from (2.8) to (2.12) we have not made any field redefinitions as done in [7]. As a result of this, the formulae in (2.12) differ from (A34) in [7] by B replaced by $-B$. This difference is a matter of choice and has no impact on physical results.

- Our results for $x_Z^{W'}$ and $x_Z^{B'}$ in (2.13) differ by signs from the ones given in (A35) of [7]. This difference is crucial for the removal of the divergences in our calculations in the unitary gauge.

- As seen in (2.17) and (2.18) we do not confirm at this order the presence of terms proportional to x_H that can be found in (A37) of [7]. Our result is consistent with the LH model with T-parity [36]-[38], where the terms proportional to x_H are also absent at this order.

2.2 The Fermion Sector

Here it suffices to state that in addition to the standard quarks and leptons there is a new heavy top quark T with the mass

$$m_T = \frac{f}{v} \frac{m_t}{\sqrt{x_L(1-x_L)}} \left(1 + \frac{v^2}{f^2}\left(\frac{1}{3} - x_L(1-x_L)\right)\right), \qquad x_L = \frac{\lambda_1^2}{\lambda_1^2 + \lambda_2^2}, \qquad (2.22)$$

where λ_1 is the Yukawa coupling in the (t, T) sector and λ_2 parametrizes the mass term for T. As already discussed in [7, 14, 18], the parameter x_L describes together with v/f the size of the violation of the three generation CKM unitarity and is also crucial for the gauge interactions of the heavy T quark with the ordinary down quarks. λ_i are expected to be $\mathcal{O}(1)$ with [7]

$$\lambda_i \geq \frac{m_t}{v}, \qquad \text{or} \qquad \frac{1}{\lambda_1^2} + \frac{1}{\lambda_2^2} \approx \left(\frac{v}{m_t}\right)^2 \qquad (2.23)$$

so that within a good approximation

$$\lambda_1 = \frac{m_t}{v}\frac{1}{\sqrt{1-x_L}}, \qquad \lambda_2 = \frac{m_t}{v}\frac{1}{\sqrt{x_L}}. \qquad (2.24)$$

x_L can in principle vary in the range $0 < x_L < 1$. However, for $x_L \approx 0$ and $x_L \approx 1$, the mass m_T will be very large and the theory will become non-perturbative. Additionally the large mass would yield a fine-tuned model, which ruins the main motivation of the theory. Varying x_L in the range $0.2 \leq x_L \leq 0.8$ and $f/v \geq 5$ as done in our paper does not induce any fine-tuning [4] and also allows us to remain in the perturbative regime.

2.3 The Charged Scalar Sector

The LH model contains also a triplet of heavy scalars of which only $\Phi^\pm$ will be of relevance here. In the case of particle-antiparticle mixing and box diagram contributions to rare decays, $\Phi^\pm$ do not contribute at $\mathcal{O}(v^2/f^2)$, but they contribute at this order to Z_L-penguin diagrams. The mass of $\Phi^\pm$ is given by

$$M_{\Phi^\pm} = \sqrt{2}m_H\frac{f}{v} \qquad (2.25)$$

with m_H denoting the light Higgs mass.

Vertex	C	Vertex	C
$W_L^+ \bar{u}_i d_j$	$\frac{ig}{2\sqrt{2}}\, V_{ij} \left(1 - \frac{v^2}{f^2}a\right)$	$W_H^+ \bar{u}_i d_j$	$-\frac{ig}{2\sqrt{2}}\, V_{ij}\frac{c}{s}\, \left(1 + b\frac{v^2}{f^2}\right)$
$W_L^+ \bar{t} d_j$	$\frac{ig}{2\sqrt{2}}\, V_{tj}\, \left(1 - \frac{v^2}{f^2}(\frac{1}{2}x_L + a)\right)$	$W_H^+ \bar{t} d_j$	$-\frac{ig}{2\sqrt{2}}\, V_{tj}\frac{c}{s}\, \left(1 - \frac{v^2}{f^2}(\frac{1}{2}x_L - b)\right)$
$W_L^+ \bar{T} d_j$	$\frac{ig}{2\sqrt{2}}\, V_{tj}\, x_L\, \frac{v}{f}\, \left(1 + \frac{v^2}{f^2}\, (d_2 - a)\right)$	$W_H^+ \bar{T} d_j$	$-\frac{ig}{2\sqrt{2}}\, V_{tj}\frac{c}{s}\, x_L\, \frac{v}{f}$

Table 1: Feynman Rules in Littlest Higgs Model for $W_{L,H}$. $C\gamma_\mu(1 - \gamma_5)$.

2.4 Feynman Rules

2.4.1 Charged Gauge Boson–Fermion Interactions

The Feynman Rules for vertices involving the charged $W_L^\pm$ and $W_H^\pm$ bosons and quarks in the notation $C\gamma_\mu(1 - \gamma_5)$ are given in table 1 where

$$a = \frac{1}{2}c^2(c^2 - s^2), \qquad b = \frac{1}{2}s^2(c^2 - s^2), \qquad d_2 = -\frac{5}{6} + \frac{1}{2}x_L^2 + 2x_L(1 - x_L). \qquad (2.26)$$

x_L is given in (2.22). For leptons the Feynman rules can be obtained from the entries of the first line with $V_{ij} = 1$. The V_{ij} are the usual CKM parameters. The issue of the violation of the CKM unitarity at $\mathcal{O}(v^2/f^2)$ has been already discussed in detail in [14] and will not be repeated here. Table 1 should be compared with table VIII of [7]. Due to different phase conventions for the t and T fields, our rules for the vertices $W_L^\pm \bar{T} d_j$ and $W_H^\pm \bar{T} d_j$ differ by a crucial factor i as already discussed in [14].

2.4.2 Neutral Gauge Boson–Fermion Interactions

The vertices involving quarks and leptons and the neutral gauge bosons Z_L^0, Z_H^0 and A_H^0, that are relevant for our paper, are presented in table 2, where g_V and g_A parametrize universally the vertices as follows

$$i\gamma_\mu(g_V + g_A\gamma_5) \qquad (2.27)$$

and

$$u = (c'^2 - s'^2), \qquad a' = \frac{1}{2}c'^2(c'^2 - s'^2). \qquad (2.28)$$

These rules follow from (A55) of [7] that we confirmed except for the signs in $x_Z^{W'}$ and $x_Z^{B'}$ in (2.13) as discussed above. In spite of agreeing with (A55) the rules presented in table 2 differ surprisingly at various places from table IX of [7]. The differences are found in the couplings $Z_L\bar{u}u$, $Z_L\bar{t}t$, $Z_L\bar{T}t$, $A_H\bar{T}T$ and $Z_H\bar{T}T$. They all are crucial for the cancellation of the divergences in our calculation. In order to make the comparison with [7] as simple as possible, table 2 has exactly the same form as the table IX of [7]. Table 2 contains also higher order terms in v/f that were required in our calculation of diagrams in classes 4 and 5 discussed below and were not present in [7].

As discussed in [7], the gauge invariance of the Yukawa interactions alone cannot unambiguously fix all the $U(1)$ charge values. The two parameters y_e and y_u that enter

the Feynman Rules in table 2 are undetermined. If one requires that the $U(1)$ charge assignments be anomaly free, they can be fixed to be

$$y_e = \frac{3}{5}, \qquad y_u = -\frac{2}{5}. \tag{2.29}$$

On the other hand, as emphasized in [7], in an effective field theory below a cutoff, it is unnecessary to be completely anomaly free as the anomalies could be cancelled by some specific extra matter at the cutoff scale. In the rest of the paper we will set y_e and y_u to the values given in (2.29) in order to avoid additional sensitivity to the physics at the cutoff scale.

We do not present the rules for the triple gauge boson vertices as they can be found in table VII of [7].

2.4.3 Charged Scalar Interactions

Only the following Feynman Rules given in [7] are of relevance in the present paper:

$$\Phi^+ \bar{u}_i d_j: \quad -\frac{i}{\sqrt{2}} \frac{g}{4} \frac{m_i}{M_{W_L}} (1 - \gamma_5) \frac{v}{f} V_{ij} \tag{2.30}$$

$$\Phi^+ \bar{T} d_j: \quad -\frac{i}{\sqrt{2}} \frac{g}{4} \frac{m_t}{M_{W_L}} (1 - \gamma_5) \frac{\lambda_1}{\lambda_2} \frac{v}{f} V_{tj} \tag{2.31}$$

$$\Phi^+ \Phi^- Z_L: \quad i\frac{g}{c_w} s_w^2 (p_+ - p_-)_\mu \tag{2.32}$$

with $p_\pm$ being outgoing momenta of $\Phi^\pm$. For the $\Phi^- \bar{d}_j u_i$ vertex $(1 - \gamma_5)$ should replaced by $(1 + \gamma_5)$ and V_{ij} by V_{ij}^*. Similarly for $\Phi^- \bar{d}_j T$.

3. X and Y in the Standard Model

Many rare decays in the SM are governed by the functions $X(x_t)$ and $Y(x_t)$ with $x_t = m_t^2/M_W^2$. It will turn out to be useful to recall the structure of the calculation of these functions. Calculating the Z^0-penguin contribution to the effective Hamiltonian for decays with $\nu\bar{\nu}$ and $\mu\bar{\mu}$ in the final state one finds

$$(\mathcal{H}_{\text{eff}}^{\nu\bar{\nu}})_Z = \frac{g^4}{64\pi^2} \frac{1}{M_Z^2 \cos^2 \theta_w} C(x_t)(\bar{s}d)_{V-A}(\bar{\nu}\nu)_{V-A}, \tag{3.1}$$

$$(\mathcal{H}_{\text{eff}}^{\mu\bar{\mu}})_Z = -\frac{g^4}{64\pi^2} \frac{1}{M_Z^2 \cos^2 \theta_w} C(x_t)(\bar{s}d)_{V-A}(\bar{\mu}\mu)_{V-A}. \tag{3.2}$$

The corresponding calculation of the box diagrams gives

$$(\mathcal{H}_{\text{eff}}^{\nu\bar{\nu}})_{\text{Box}} = \frac{g^4}{64\pi^2} \frac{1}{M_W^2} B^{\nu\bar{\nu}}(x_t)(\bar{s}d)_{V-A}(\bar{\nu}\nu)_{V-A}, \tag{3.3}$$

$$(\mathcal{H}_{\text{eff}}^{\mu\bar{\mu}})_{\text{Box}} = -\frac{g^4}{64\pi^2} \frac{1}{M_W^2} B^{\mu\bar{\mu}}(x_t)(\bar{s}d)_{V-A}(\bar{\mu}\mu)_{V-A}. \tag{3.4}$$

vertex	g_V	g_A
$A_L\bar{f}f$	$-eQ_f$	0
$Z_L\bar{u}u$	$-\frac{g}{2c_w}\left\{\left(\frac{1}{2}-\frac{4}{3}s_w^2\right)-\frac{v^2}{f^2}\left[c_w x_Z^{W'}c/2s \right.\right.$ $\left.\left.+\frac{s_w x_Z^{B'}}{s'c'}\left(2y_u+\frac{17}{15}-\frac{5}{6}c'^2\right)\right]\right\}$	$-\frac{g}{2c_w}\left\{-\frac{1}{2}-\frac{v^2}{f^2}\left[-c_w x_Z^{W'}c/2s \right.\right.$ $\left.\left.+\frac{s_w x_Z^{B'}}{s'c'}\left(\frac{1}{5}-\frac{1}{2}c'^2\right)\right]\right\}$
$Z_L\bar{d}d$	$-\frac{g}{2c_w}\left\{\left(-\frac{1}{2}+\frac{2}{3}s_w^2\right)-\frac{v^2}{f^2}\left[-c_w x_Z^{W'}c/2s \right.\right.$ $\left.\left.+\frac{s_w x_Z^{B'}}{s'c'}\left(2y_u+\frac{11}{15}+\frac{1}{6}c'^2\right)\right]\right\}$	$-\frac{g}{2c_w}\left\{\frac{1}{2}-\frac{v^2}{f^2}\left[c_w x_Z^{W'}c/2s \right.\right.$ $\left.\left.+\frac{s_w x_Z^{B'}}{s'c'}\left(-\frac{1}{5}+\frac{1}{2}c'^2\right)\right]\right\}$
$Z_L\bar{e}e$	$-\frac{g}{2c_w}\left\{\left(-\frac{1}{2}+2s_w^2\right)-\frac{v^2}{f^2}\left[-c_w x_Z^{W'}c/2s \right.\right.$ $\left.\left.+\frac{s_w x_Z^{B'}}{s'c'}\left(2y_e-\frac{9}{5}+\frac{3}{2}c'^2\right)\right]\right\}$	$-\frac{g}{2c_w}\left\{\frac{1}{2}-\frac{v^2}{f^2}\left[c_w x_Z^{W'}c/2s \right.\right.$ $\left.\left.+\frac{s_w x_Z^{B'}}{s'c'}\left(-\frac{1}{5}+\frac{1}{2}c'^2\right)\right]\right\}$
$Z_L\bar{\nu}\nu$	$-\frac{g}{2c_w}\left\{\frac{1}{2}-\frac{v^2}{f^2}\left[c_w x_Z^{W'}c/2s \right.\right.$ $\left.\left.+\frac{s_w x_Z^{B'}}{s'c'}\left(y_e-\frac{4}{5}+\frac{1}{2}c'^2\right)\right]\right\}$	$-\frac{g}{2c_w}\left\{-\frac{1}{2}-\frac{v^2}{f^2}\left[-c_w x_Z^{W'}c/2s \right.\right.$ $\left.\left.+\frac{s_w x_Z^{B'}}{s'c'}\left(-y_e+\frac{4}{5}-\frac{1}{2}c'^2\right)\right]\right\}$
$Z_L\bar{t}t$	$-\frac{g}{2c_w}\left\{\left(\frac{1}{2}-\frac{4}{3}s_w^2\right)-\frac{v^2}{f^2}\left[x_L^2/2+c_w x_Z^{W'}c/2s \right.\right.$ $\left.\left.+\frac{s_w x_Z^{B'}}{s'c'}\left(2y_u+\frac{17}{15}-\frac{5}{6}c'^2-\frac{1}{5}\frac{\lambda_1^2}{\lambda_1^2+\lambda_2^2}\right)\right]\right\}$	$-\frac{g}{2c_w}\left\{-\frac{1}{2}-\frac{v^2}{f^2}\left[-x_L^2/2-c_w x_Z^{W'}c/2s \right.\right.$ $\left.\left.+\frac{s_w x_Z^{B'}}{s'c'}\left(\frac{1}{5}-\frac{1}{2}c'^2-\frac{1}{5}\frac{\lambda_1^2}{\lambda_1^2+\lambda_2^2}\right)\right]\right\}$
$Z_L\bar{T}T$	$\frac{g}{2c_w}\left\{\frac{4}{3}s_w^2+\frac{v^2}{f^2}\left(-\frac{1}{2}x_L^2+\right.\right.$ $\left.\left.\frac{s_w x_Z^{B'}}{s'c'}(2y_u+\frac{14}{15}-\frac{4}{3}c'^2+\frac{1}{5}x_L)\right)\right\}$	$\frac{g}{2c_w}\frac{v^2}{f^2}\left\{\frac{1}{2}x_L^2+\frac{s_w x_Z^{B'}}{s'c'}\frac{1}{5}x_L\right\}$
$Z_L\bar{T}t$	$\frac{g}{2c_w}\left\{-\frac{v}{f}\frac{1}{2}x_L+\frac{v^2}{f^2}\frac{s_w x_Z^{B'}}{c's'}\left(\frac{1}{5}x_L\frac{\lambda_2}{\lambda_1}\right)+\right.$ $\left.\frac{v^3}{f^3}\left(\frac{1}{4}x_L^3-\frac{1}{2}x_L d_2+x_L(\frac{c'}{s'}\frac{s_w x_Z^{B'}}{2}+\frac{c}{s}\frac{c_w x_Z^{W'}}{2})\right)\right\}$	$\frac{g}{2c_w}\left\{\frac{v}{f}\frac{1}{2}x_L+\frac{v^2}{f^2}\frac{s_w x_Z^{B'}}{c's'}\left(\frac{1}{5}x_L\frac{\lambda_2}{\lambda_1}\right)+\right.$ $\left.\frac{v^3}{f^3}\left(-\frac{1}{4}x_L^3+\frac{1}{2}x_L d_2-x_L(\frac{c'}{s'}\frac{s_w x_Z^{B'}}{2}+\frac{c}{s}\frac{c_w x_Z^{W'}}{2})\right)\right\}$
$A_H\bar{u}u$	$\frac{g'}{2s'c'}\left(2y_u+\frac{17}{15}-\frac{5}{6}c'^2\right)$	$\frac{g'}{2s'c'}\left(\frac{1}{5}-\frac{1}{2}c'^2\right)$
$A_H\bar{d}d$	$\frac{g'}{2s'c'}\left(2y_u+\frac{11}{15}+\frac{1}{6}c'^2\right)$	$\frac{g'}{2s'c'}\left(-\frac{1}{5}+\frac{1}{2}c'^2\right)$
$A_H\bar{e}e$	$\frac{g'}{2s'c'}\left(2y_e-\frac{9}{5}+\frac{3}{2}c'^2\right)$	$\frac{g'}{2s'c'}\left(-\frac{1}{5}+\frac{1}{2}c'^2\right)$
$A_H\bar{\nu}\nu$	$\frac{g'}{2s'c'}\left(y_e-\frac{4}{5}+\frac{1}{2}c'^2\right)$	$\frac{g'}{2s'c'}\left(-y_e+\frac{4}{5}-\frac{1}{2}c'^2\right)$
$A_H\bar{t}t$	$\frac{g'}{2s'c'}\left(2y_u+\frac{17}{15}-\frac{5}{6}c'^2-\frac{1}{5}\frac{\lambda_1^2}{\lambda_1^2+\lambda_2^2}\right)$	$\frac{g'}{2s'c'}\left(\frac{1}{5}-\frac{1}{2}c'^2-\frac{1}{5}\frac{\lambda_1^2}{\lambda_1^2+\lambda_2^2}\right)$
$A_H\bar{T}T$	$\frac{g'}{2s'c'}\left(2y_u+\frac{14}{15}-\frac{4}{3}c'^2+\frac{1}{5}\frac{\lambda_1^2}{\lambda_1^2+\lambda_2^2}\right)$	$\frac{g'}{2s'c'}\frac{1}{5}\frac{\lambda_1^2}{\lambda_1^2+\lambda_2^2}$
$A_H\bar{T}t$	$\frac{g'}{2s'c'}\left(\frac{1}{5}x_L\frac{\lambda_2}{\lambda_1}+\frac{v}{f}\frac{1}{2}c'^2 x_L\right)$	$\frac{g'}{2s'c'}\left(\frac{1}{5}x_L\frac{\lambda_2}{\lambda_1}-\frac{v}{f}\frac{1}{2}c'^2 x_L\right)$
$Z_H\bar{u}u$	$gc/4s$	$-gc/4s$
$Z_H\bar{d}d$	$-gc/4s$	$gc/4s$
$Z_H\bar{e}e$	$-gc/4s$	$gc/4s$
$Z_H\bar{\nu}\nu$	$gc/4s$	$-gc/4s$
$Z_H\bar{t}t$	$gc/4s$	$-gc/4s$
$Z_H\bar{T}T$	$\mathcal{O}(v^2/f^2)$	$\mathcal{O}(v^2/f^2)$
$Z_H\bar{T}t$	$gx_L vc/4fs$	$-gx_L vc/4fs$

Table 2: Feynman Rules in LH Model for Z_L, A_H and Z_H. g_V and g_A defined in (2.27).

Adding the Z^0-penguin and box contributions and using the relations

$$M_Z^2 \cos^2 \theta_w = M_W^2, \qquad \frac{G_F}{\sqrt{2}} = \frac{g^2}{8M_W^2} \tag{3.5}$$

one arrives at

$$\mathcal{H}_{\text{eff}}^{\nu\bar{\nu}} = M_W^2 \frac{G_F^2}{2\pi^2} X(x_t)(\bar{s}d)_{V-A}(\bar{\nu}\nu)_{V-A}, \tag{3.6}$$

$$\mathcal{H}_{\text{eff}}^{\mu\bar{\mu}} = -M_W^2 \frac{G_F^2}{2\pi^2} Y(x_t)(\bar{s}d)_{V-A}(\bar{\mu}\mu)_{V-A}, \tag{3.7}$$

where

$$X(x_t) = C(x_t) + B^{\nu\bar{\nu}}(x_t), \qquad Y(x_t) = C(x_t) + B^{\mu\bar{\mu}}(x_t). \tag{3.8}$$

It is customary to use in (3.6) and (3.7) the relation

$$M_W^2 \frac{G_F^2}{2\pi^2} = \frac{G_F}{\sqrt{2}} \frac{\alpha}{2\pi \sin^2 \theta_w}, \tag{3.9}$$

but we will not use it here for reasons discussed in the next section.

Now, $C(x_t)$, $B^{\nu\bar{\nu}}(x_t)$ and $B^{\mu\bar{\mu}}(x_t)$ depend on the gauge used for the $W^\pm$ propagator. One has [28, 29]

$$C(x_t) = C_0(x_t) + \frac{1}{2}\bar{\varrho}(x_t) \tag{3.10}$$

$$B^{\nu\bar{\nu}}(x_t) = -4B_0(x_t) - \frac{1}{2}\bar{\varrho}(x_t), \qquad B^{\mu\bar{\mu}}(x_t) = -B_0(x_t) - \frac{1}{2}\bar{\varrho}(x_t), \tag{3.11}$$

where $\bar{\varrho}(x_t)$ is gauge dependent with $\bar{\varrho}(x_t) = 0$ in the Feynman–t'Hooft gauge and

$$B_0(x_t) = \frac{1}{4}\left[\frac{x_t}{1 - x_t} + \frac{x_t \log x_t}{(x_t - 1)^2}\right], \tag{3.12}$$

$$C_0(x_t) = \frac{x_t}{8}\left[\frac{x_t - 6}{x_t - 1} + \frac{3x_t + 2}{(x_t - 1)^2} \log x_t\right] . \tag{3.13}$$

Evidently $X(x_t)$ and $Y(x_t)$ are gauge independent and given in the SM as follows:

$$X(x_t) = \frac{x_t}{8}\left[\frac{x_t + 2}{x_t - 1} + \frac{3x_t - 6}{(x_t - 1)^2} \log x_t\right], \tag{3.14}$$

$$Y(x_t) = \frac{x_t}{8}\left[\frac{x_t - 4}{x_t - 1} + \frac{3x_t}{(x_t - 1)^2} \log x_t\right]. \tag{3.15}$$

Explicit expression for $\bar{\varrho}(x_t)$ in an arbitrary R_ξ gauge can be found in [28, 29]. In the LH model we will calculate X and Y in the unitary gauge and we will need at one stage the SM function $C(x_t)$ in this gauge. As the penguin and box diagrams are divergent in the unitary gauge, even after the GIM mechanism has been invoked, we use the dimensional regularization with $D = 4 - 2\varepsilon$ to find

$$C(x_t)_{\text{unitary}} = -\frac{1}{16}x_t\left(\frac{1}{\varepsilon} + \ln\frac{\mu^2}{M_{W_L}^2}\right) - \frac{x_t^2 - 7x_t}{32(1 - x_t)} + \frac{4x_t - 2x_t^2 + x_t^3}{16(1 - x_t)^2} \log x_t \tag{3.16}$$
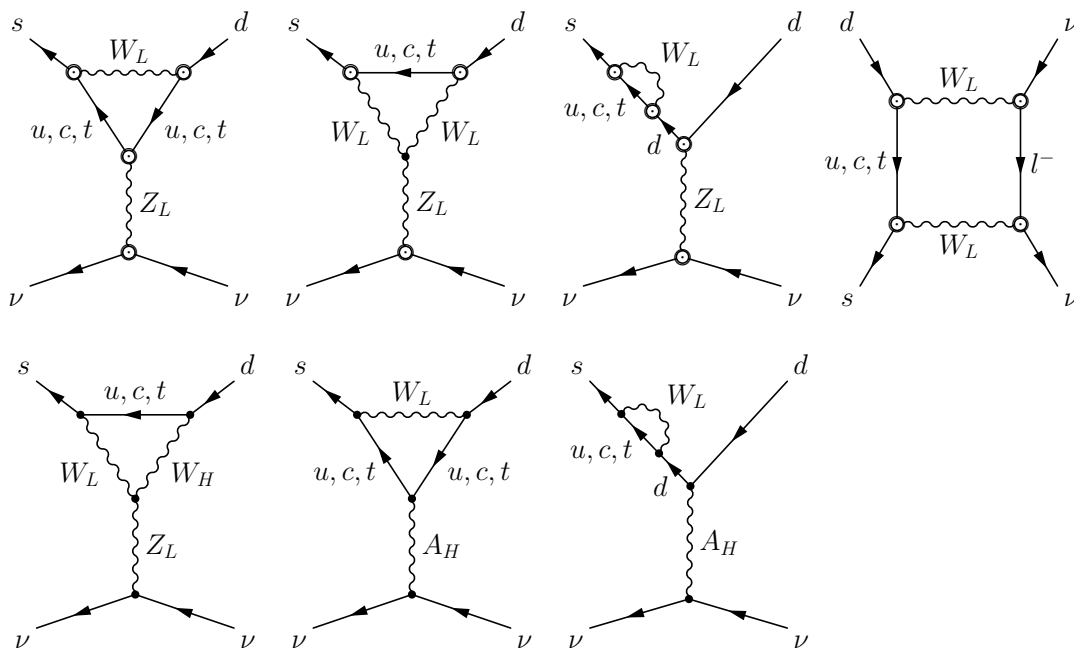
Figure 1: Class 1. Penguin and box diagrams with SM particles and A_H contributing to $K \to \pi\nu\bar{\nu}$ within the LH model at $\mathcal{O}(v^2/f^2)$.

and

$$\bar{\varrho}(x_t)_{\text{unitary}} = -\frac{1}{8}x_t\left(\frac{1}{\varepsilon} + \ln\frac{\mu^2}{M_{W_L}^2}\right) - \frac{-3x_t^2 + 17x_t}{16(1-x_t)} - \frac{8x_t^2 - x_t^3}{8(x_t-1)^2}\log x_t \ . \qquad (3.17)$$

The $\ln\left(\mu^2/M_{W_L}^2\right)$ terms disappear in the final expressions for X and Y as they always accompany $1/\varepsilon$ that is not present in X and Y in the SM.

4. X and Y in the Littlest Higgs Model

4.1 Six Classes of Diagrams

In the LH model the functions X and Y are modified through the contributions of new penguin and box diagrams involving the heavy fields W_H, Z_H, A_H, T and $\Phi^\pm$. In order to show transparently how the cancellation of most of the divergences takes place, it is useful to group the diagrams contributing at $\mathcal{O}(v^2/f^2)$ into six distinct classes which are shown in figures 1–6.

Class 1, displayed in figure 1, summarizes all diagrams with exclusively Standard Model particles. The circles around the vertices of these diagrams indicate that the $\mathcal{O}(v^2/f^2)$ corrections to their vertices *without* the x_L^2 terms are considered. Using the leading order vertices one arrives at the SM $X(x_t)$ function. Furthermore, the $W_L W_H Z_L$ triple vertex and the (W_L, A_H) penguin diagrams with the standard top quark propagating belong to this class.
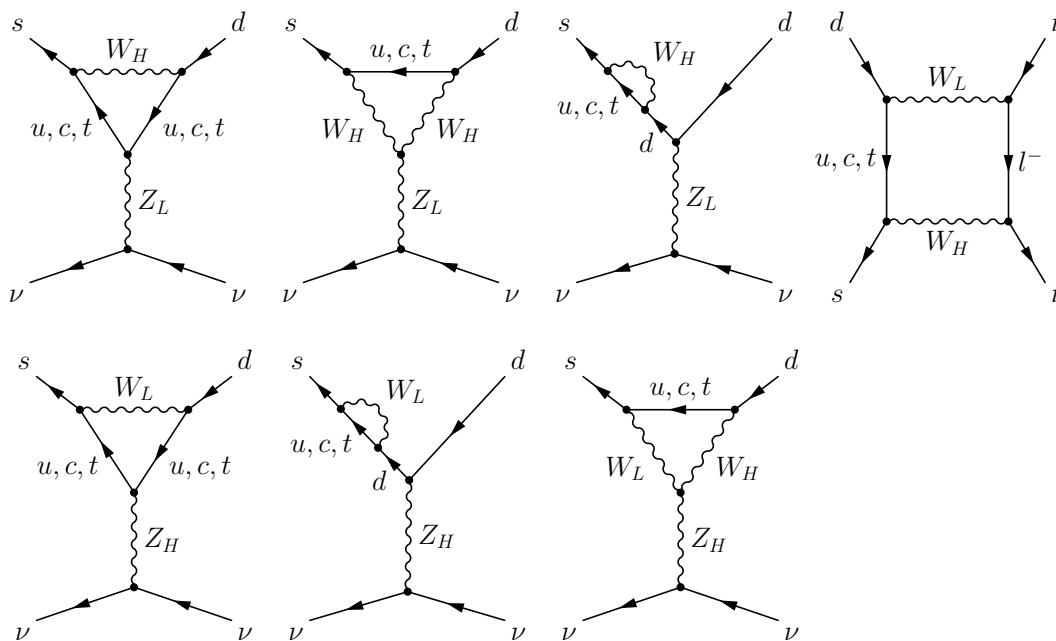
Figure 2: Class 2. Penguin and box diagrams with W_H and Z_H contributing to $K \to \pi \nu \bar{\nu}$ within the LH model at $\mathcal{O}(v^2/f^2)$.

Class 2 contains the contributions of the standard top quark in the (W_H, Z_L) and (W_L, Z_H) penguin diagrams, the (W_L, W_H) box diagram and the diagrams with the $W_L W_H Z_H$ and $W_H W_H Z_L$ triple vertices that are of order v^2/f^2. The whole contribution of this class is proportional to the parameter c^4.

The penguin and box diagrams involving the heavy T quark as well as the contributions of the standard top quark that are proportional to x_L^2 are displayed in figure 3 and belong to Class 3. The vertices of the standard top quark are marked by the diamonds in this figure which implies that here the terms in the vertices proportional to x_L^2, excluded from Class 1, are considered. The approximate results for this class have been already presented in [18]. Here we present exact formulae at $\mathcal{O}(v^2/f^2)$.

The divergences of Class 3 involving the heavy top quark T are proportional to $v^2/f^2 x_T/\varepsilon$. As the mass of the heavy T is of order f/v, these singularities are of $\mathcal{O}(1)$. This makes clear that diagrams with singularities of the type $v^4/f^4 x_T/\varepsilon$ also have to be considered and it turns out that the inclusion of these divergences is essential for the removal of the singularities of the whole $\mathcal{O}(v^2/f^2)$ result except for the singularities discussed in Section 5. The relevant contributions of this type containing the heavy top quark T and being suppressed by v^4/f^4 are summarized in Class 4 and Class 5. Class 4 is very similar to Class 2 with the standard top quark replaced by the heavy top quark and additional two diagrams with t and T exchanges. Class 5 contains diagrams of Class 1 with t replaced by T in the first five diagrams in Fig. 5 and with corrections added to the last five diagrams in figure 3 as explicitly indicated in figure 5.
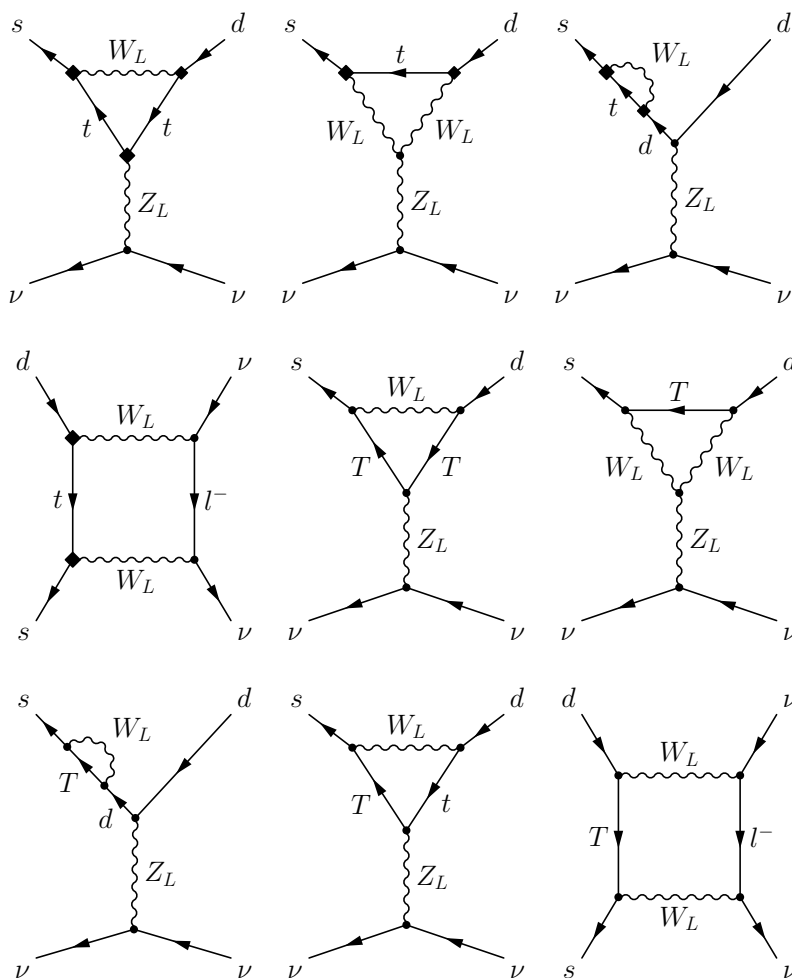
Figure 3: Class 3. Top and heavy top quark contributions to $K \to \pi\nu\bar{\nu}$ in the LH model at $\mathcal{O}(v^2/f^2)$ which are proportional to x_L^2.

In the previous section we pointed out that due to the breakdown of the custodial $SU(2)$ symmetry at $\mathcal{O}(v^2/f^2)$ in the LH model, the SM relation (3.5) is replaced by (2.20). In the process of expressing M_Z in the Z-penguin in terms of M_W all contributions of $\mathcal{O}(1)$ belonging to Z_L vertices obtain $\mathcal{O}(v^2/f^2)$ corrections. Explicitly, corrections to the contribution of the SM penguin diagrams of Class 1 and Z_L penguins with heavy top quark T of Class 3 arise. We find then two additional contributions

$$\Delta X_{\text{Custodial 1}} = \Delta Y_{\text{Custodial 1}} = \frac{v^2}{f^2} \frac{5}{4} (c'^2 - s'^2)^2 C(x_t)_{\text{unitary}}, \tag{4.1}$$

$$\Delta X_{\text{Custodial 3}} = \Delta Y_{\text{Custodial 3}} = \frac{v^4}{f^4} \frac{5}{4} (c'^2 - s'^2)^2 x_L^2 C(x_T)_{\text{Class 3}}, \tag{4.2}$$
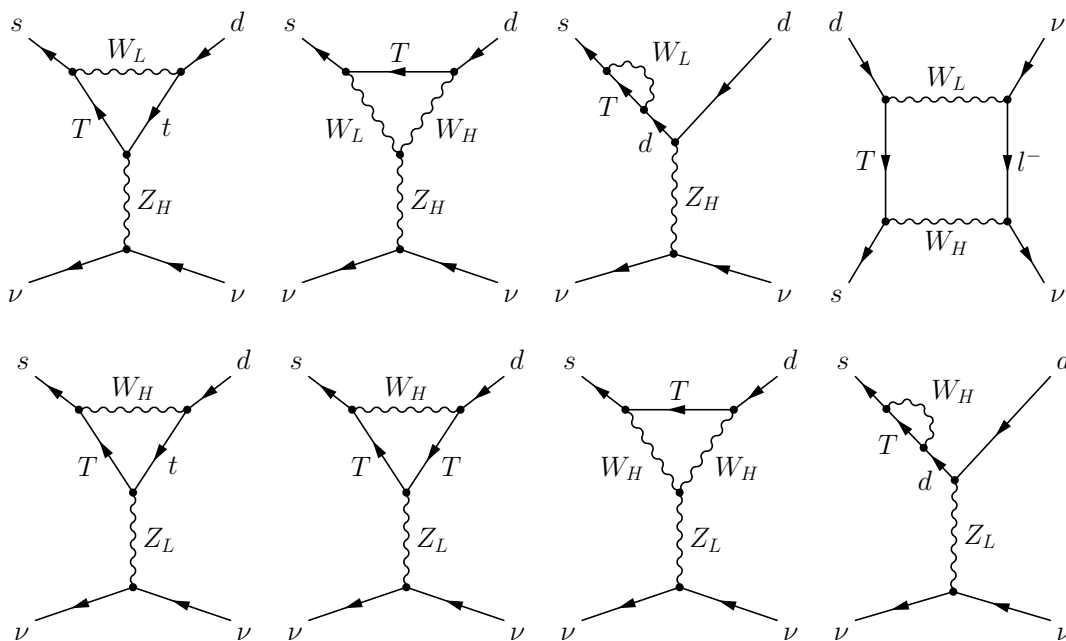
Figure 4: Class 4. Penguin and box contributions to $K \to \pi\nu\bar{\nu}$ in the LH model at $\mathcal{O}(v^2/f^2)$ which are proportional to $v^4/f^4 c^4 x_L^2$.

with $C(x_t)_{\text{unitary}}$ given in (3.16). For $C(x_T)_{\text{Class}\,3}$ we obtain

$$C(x_T)_{\text{Class}\,3} = -\frac{x_T}{16}\left(\frac{1}{\varepsilon} + \ln\frac{\mu^2}{M_{W_L}^2}\right) - \frac{3x_T}{32} + \frac{(-2 + x_T)\log x_T}{16}. \tag{4.3}$$

It has to be emphasized that the inclusion of these two corrections resulting from the breakdown of custodial symmetry in the LH model is essential for the removal of the s' dependence as we will show in the next section and removes some divergences.

Finally in figure 6 we show the diagrams involving $\Phi^\pm$ that contribute at $\mathcal{O}(v^2/f^2)$.

4.2 Analytic Results

In order to explicitly show how the divergences cancel, we list in Appendix B the singularities in Class 1 to 3 in table 4, and the ones of Class 4 and 5 in table 5. The singularities in Class 6 are listed in table 6. The entries of each class are arranged according to the position of the corresponding diagrams in Figs. 1–6. The variables a, d_2, u and a' are defined in (2.26) and (2.28).

The divergences in Class 2, Class 3 and Class 4 cancel separately within each class. For the classes 1, 5 and 6 the situation is a bit different. Some divergences of Class 1 and Class 5 can only be removed in the sum of the singularities of both classes together with the inclusion of the singularities due to the breakdown of the custodial $SU(2)$ symmetry,

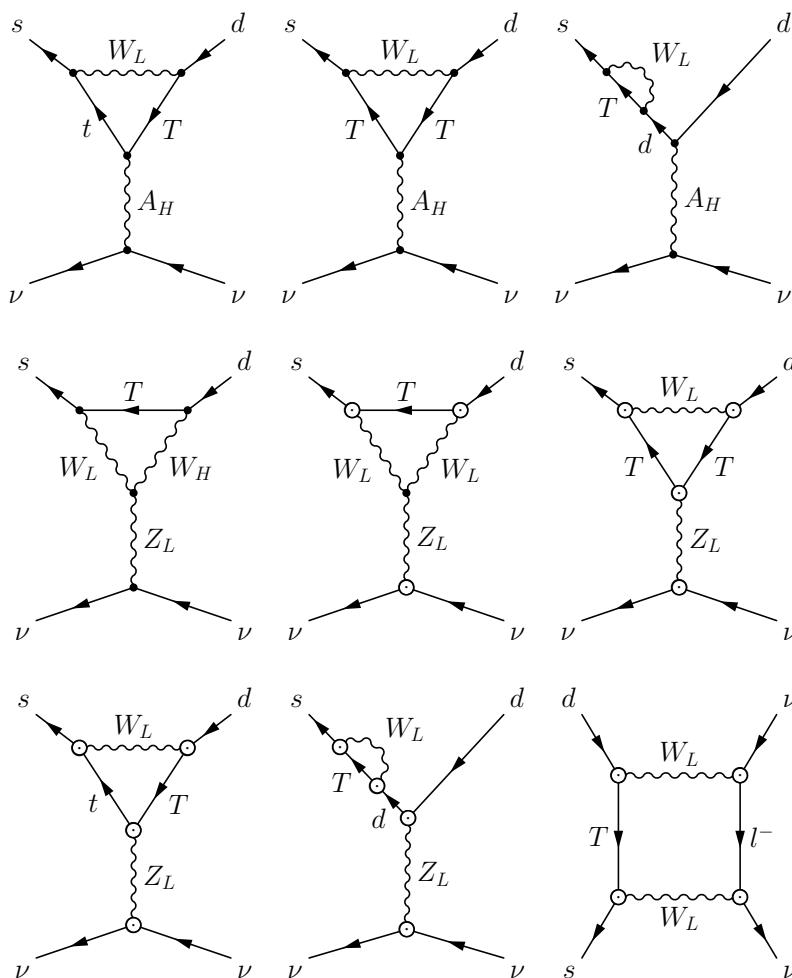$$\frac{x_t}{\varepsilon}\frac{v^2}{f^2}\left(-\frac{5}{64}(c'^2 - s'^2)^2\right), \tag{4.4}$$

Figure 5: Class 5. Penguin and box contributions to $K \to \pi \nu \bar{\nu}$ in the LH model at $\mathcal{O}(v^2/f^2)$ which are proportional to $v^4/f^4 x_T x_L^2$.

$$\frac{x_T}{\varepsilon} \frac{v^4}{f^4} x_L^2 \left(-\frac{5}{64} (c'^2 - s'^2)^2 \right),$$
(4.5)

which are also shown in table 4 and 5, respectively and can be obtained from (4.1) and (4.2). Further on, singularities of the standard top quark are canceled by those of the heavy top quark with the use of relation (2.22) as

$$x_L^2 \frac{x_T}{\varepsilon} = \frac{x_L}{1 - x_L} \frac{x_t}{\varepsilon} \frac{f^2}{v^2}.$$
(4.6)

However, as already stated at the beginning of our paper singularities from classes 1 and 5 and the charged Higgs diagrams of figure 6 are left. We find

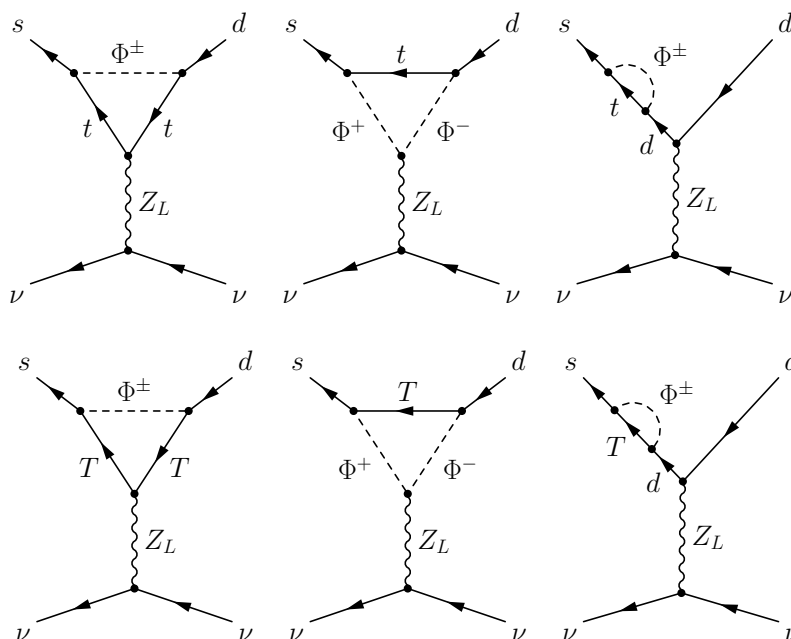$$C_{\text{div}} = \frac{x_t}{64} \frac{1}{1 - x_L} \frac{v^2}{f^2} \left(-\frac{S_1}{5} + S_2 \right),$$
(4.7)

Figure 6: Class 6. Penguin contributions to $K \to \pi \nu \bar\nu$ in the LH model at $\mathcal{O}(v^2/f^2)$ with internal charged scalars $\Phi^\pm$.

where

$$S_1 = \frac{1}{\varepsilon} + \ln \frac{\mu^2}{M_{W_L}^2} \qquad \text{and} \qquad S_2 = \frac{1}{\varepsilon} + \ln \frac{\mu^2}{M_\Phi^2}. \tag{4.8}$$

S_1 results from classes 1 and 5 and S_2 from charged Higgs diagrams. We will return to discuss these singularities in the next Section. We caution the reader that the logarithms associated with $1/\varepsilon$ have not been explicitly shown in tables 4-6.

We can then write the results for X and Y in the LH model as

$$X_{\text{LH}}(x_t, z) = X_{\text{SM}}(x_t) + \Delta X_1 + \Delta X_2 + \Delta X_3 + \Delta X_4 + \Delta X_5 + \Delta X_6 \tag{4.9}$$

$$Y_{\text{LH}}(x_t, z) = Y_{\text{SM}}(x_t) + \Delta Y_1 + \Delta Y_2 + \Delta Y_3 + \Delta Y_4 + \Delta Y_5 + \Delta Y_6 \tag{4.10}$$

where z denotes collectively the parameters in the LH model to which we will return below. The finite parts of the two corrections due to the custodial relation given by (4.1) and (4.2) were included into the X and Y functions of Class 1 and Class 5. We emphasize, that once these corrections are included the dependence on s' drops out.

For the six classes in question we find

$$\Delta X_1 = \frac{v^2}{f^2} U_1, \qquad \Delta X_2 = c^4 \frac{v^2}{f^2} U_2 \quad = \frac{c^2}{s^2} \frac{1}{y} U_2, \tag{4.11}$$

$$\Delta X_3 = x_L^2 \frac{v^2}{f^2} U_3, \qquad \Delta X_4 = x_L^2 c^4 \frac{v^4}{f^4} U_4 = x_L^2 \frac{c^2}{s^2} \frac{1}{y} \frac{v^2}{f^2} U_4, \tag{4.12}$$

$$\Delta X_5 = x_L^2 \frac{v^4}{f^4} U_5, \qquad \Delta X_6 = \frac{v^2}{f^2} \frac{x_t}{128} \frac{1}{1 - x_L} (1 - 2x_L U_6(\hat{x}_T)) \tag{4.13}$$

– 18 –

$$\Delta Y_1 = \frac{v^2}{f^2}\, V_1, \qquad\qquad \Delta Y_2 = c^4 \frac{v^2}{f^2}\, V_2 \quad = \frac{c^2}{s^2}\frac{1}{y} V_2, \tag{4.14}$$

$$\Delta Y_3 = x_L^2\, \frac{v^2}{f^2}\, V_3, \qquad\qquad \Delta Y_4 = x_L^2 c^4 \frac{v^4}{f^4} V_4 = x_L^2 \frac{c^2}{s^2}\frac{1}{y}\frac{v^2}{f^2}\, V_4, \tag{4.15}$$

$$\Delta Y_5 = x_L^2 \frac{v^4}{f^4}\, V_5 \qquad\qquad \Delta Y_6 = \Delta X_6 \tag{4.16}$$

with

$$U_1(x_t, y) = -\frac{(1+4x_L)\, x_t}{320} S_1 + \frac{(1+4x_L)\,(-7+x_t)\, x_t}{640\,(-1+x_t)}$$
$$+ \frac{(1+4x_L)\, x_t \left(4 - 2x_t + x_t^2\right)\log x_t}{320\,(-1+x_t)^2}$$
$$- \frac{ax_t\,(11+4x_t)}{8\,(-1+x_t)} - \frac{3ax_t\left(-8+2x_t+x_t^2\right)\log x_t}{8\,(-1+x_t)^2} + \frac{3ax_t\log y}{8} \tag{4.17}$$

$$U_2(x_t, y) = -\frac{x_t\,(4-7x_t)}{16(-1+x_t)} - \frac{3x_t\left(8-6x_t-x_t^2\right)\log x_t}{16(-1+x_t)^2} - \frac{x_t \log y}{4} \tag{4.18}$$

$$U_3(x_t, x_T) = \frac{-3+2x_t-2x_t^2}{8(-1+x_t)} - \frac{x_t\left(-4-x_t+2x_t^2\right)\log x_t}{8(-1+x_t)^2} + \frac{(3+2x_t)\log x_T}{8} \tag{4.19}$$

$$U_4(x_T, y) = \frac{3x_T y}{16\,(-x_T+y)} + \frac{3x_T y^2 \log x_T}{16(x_T-y)^2} - \frac{3x_T y^2 \log y}{16(x_T-y)^2} - \frac{x_T \log y}{16} \tag{4.20}$$

$$U_5(x_t, x_T) = -\frac{(-3+4x_L)\, x_T}{320} S_1 + \frac{\left(-7-12x_L+80x_L^2\right)x_T}{640} + \frac{(-3+4x_L)\, x_T \log x_T}{320}$$
$$+ \frac{3ax_T y\,(\log x_T - \log y)}{8\,(x_T-y)} \tag{4.21}$$

$$U_6(\hat{x}_T) = -\frac{S_2}{x_L} + \frac{\hat{x}_T}{(1-\hat{x}_T)} + \frac{\hat{x}_T^2 \log \hat{x}_T}{(1-\hat{x}_T)^2} \tag{4.22}$$

$$V_1(x_t, y) = -\frac{(1+4x_L)\, x_t}{320} S_1 + \frac{(1+4x_L)\,(-7+x_t)\, x_t}{640\,(-1+x_t)}$$
$$+ \frac{(1+4x_L)\, x_t \left(4 - 2x_t + x_t^2\right)\log x_t}{320\,(-1+x_t)^2}$$
$$- \frac{ax_t\,(-13+4x_t)}{8\,(-1+x_t)} - \frac{3ax_t^2\,(2+x_t)\log x_t}{8\,(-1+x_t)^2} + \frac{3ax_t\log y}{8} \tag{4.23}$$

$$V_2(x_t, y) = -\frac{x_t\,(4-7x_t)}{16(-1+x_t)} - \frac{3x_t^2\,(2-x_t)\log x_t}{16(-1+x_t)^2} - \frac{x_t \log y}{4} \tag{4.24}$$

$$V_3(x_t, x_T) = \frac{\left(3+2x_t-2x_t^2\right)}{8(-1+x_t)} - \frac{x_t\left(2-x_t+2x_t^2\right)\log x_t}{8(-1+x_t)^2} + \frac{(3+2x_t)\log x_T}{8} \tag{4.25}$$

$$V_4(x_T, y) = \frac{3x_T y}{16\,(-x_T+y)} + \frac{3x_T y^2 \log x_T}{16(x_T-y)^2} - \frac{3x_T y^2 \log y}{16(x_T-y)^2} - \frac{x_T \log y}{16} \tag{4.26}$$

$$V_5(x_t, x_T) = -\frac{(-3+4x_L)\,x_T}{320}S_1 + \frac{(-7-12x_L+80x_L^2)\,x_T}{640} + \frac{(-3+4x_L)\,x_T\log x_T}{320}$$
$$+ \frac{3ax_Ty\,(\log x_T - \log y)}{8\,(x_T - y)}, \tag{4.27}$$

where S_1 and S_2 have been defined in (4.8) and

$$x_i = \frac{m_i^2}{M_{W_L^\pm}^2}, \qquad y = \frac{M_{W_H^\pm}^2}{M_{W_L^\pm}^2}, \qquad \hat{x}_T = \frac{m_T^2}{M_{\Phi^\pm}^2}. \tag{4.28}$$

In our calculations, we considered all contributions to the order v^2/f^2. This implies the neglection of higher order terms in the functions U_i and V_i. As explained above, Class 4 and Class 5 even if suppressed by v^4/f^4 factors, contribute to the order considered as they depend on heavy masses and $x_T, y \propto f^2/v^2$.

The formulae for ΔX_i and ΔY_i presented above are the main results of our paper.

5. The Issue of Leftover Singularities

It may seem surprising that FCNC amplitudes considered in the previous section contain residual ultraviolet divergences reflected by the non-cancellation of the $1/\varepsilon$ poles at $\mathcal{O}(v^2/f^2)$ in our unitary gauge calculation. Indeed due to GIM mechanism the FCNC processes considered here vanish at tree level both in the SM and in the LH model in question. Therefore within the particle content of the low energy representation of the LH model there seems to be no freedom to cancel the left-over divergences as the necessary tree level counter terms are absent.

At first sight then one could worry that the remaining divergence is an artifact of the unitary gauge calculation. However, the fact that the dominant divergence comes from the gauge independent charged triplet Higgs $\Phi^\pm$ contribution gives us a hint that the residual divergence is not an artifact of the unitary gauge but reflects the true sensitivity to the UV completion of the LH model and the presence of additional contributions to the non-linear sigma model used as the effective field theory at low energy.

In order to put this hypothesis on a solid ground we have analyzed the divergent part of the amplitudes in the Feynman gauge. Then the box diagram contributions are finite and it is sufficient to concentrate on the penguin (vertex) contributions. In this context let us recall that in the SM the divergent contributions from penguin diagrams involving only quarks and gauge bosons are removed by the GIM mechanism as the divergent terms are mass independent. Some of the vertex diagrams with internal Goldstone bosons are also divergent and being proportional to $m_i^2, (i = u, d, t)$ these divergences cannot be removed by GIM mechanism. Within the SM they cancel, however, due to gauge invariance and renormalizability of the theory.

In the LH model in Feynman gauge there are no divergences left from the pure gauge boson diagrams of classes 1-5 shown in figures 1–5. Note also that the divergence from the breakdown of the custodial symmetry is also absent as in the Feynman gauge, as seen in (3.13), the SM function C is finite. Thus the left-over divergences come only from the

charged triplet Higgs contribution in figure 6 and two charged Goldstone bosons that now have to be included in the evaluation of the diagrams of classes 1-5. These are a charged vector Higgs boson which is responsible for the mass of W_H and the usual charged doublet Higgs boson which gives mass to W_L. We confirm that the left-over divergence coming from these Goldstone boson contributions to classes 1-5 exactly reproduces the divergence discovered in the corresponding unitary gauge calculation. Combined with the charged triplet Higgs contribution we reproduce, in Feynman gauge, the full divergence of (4.7).

To understand the meaning of these ultraviolet divergences it is important to recall that the LH model is a non-linear sigma model, an effective field theory that describes the low energy behavior of a symmetric theory below the scale where the symmetry is dynamically broken. In this region the currents associated with the dynamically broken generators are conserved by a cancellation between the quark charge form factor current and the Goldstone current. Quark currents will remain conserved even when the charge form factor is renormalized so long as the Yukawa coupling of the Goldstone bosons to the fermions has a corresponding renormalization. It is easy to confirm that this is exactly what happens in the non-linear sigma model used above to describe the Little Higgs theory and the divergence may be identified as a renormalization of the quark charges associated with neutral current processes. The subsequent gauging of the Little Higgs theory only rearranges the infrared structure of the theory but cannot modify the ultraviolet behavior. The divergence in the charge form factors is not a true ultraviolet divergence but reflects sensitivity to the UV completion of the theory.

This same mechanism can be observed in the phenomenological description of dynamical chiral symmetry breaking in QCD using a non-linear realization of the pseudo-scalar mesons as Goldstone bosons. Here the axial charges are dynamically broken but the axial vector currents remain conserved due to the Goldstone currents of pions. To apply this theory to the physical baryons, the axial charge of the baryon is observed to be renormalized, $G_A \sim 1.26 \neq 1$. This renormalization is consistent with a conserved axial vector current so long as the Goldstone coupling of the pions to the baryons is modified according to the Goldberger-Treiman relation. In fact, the naive constituent quark model predicts an even larger value of 5/3 for the axial charge of the baryon where the axial charge of the quark is taken to be 1. As mentioned in the introduction, Peris [26] has considered the next-to-leading order chiral loop corrections to the axial charge form factors of the constituent quark. He uses a linear sigma model to regularize the non-linear theory and finds a logarithmic sensitivity to the mass of the scalar partners to the pions reflecting the chiral splitting within the meson multiplet. In the non-linear version, his calculation would generate logarithmic divergences exactly analogous to the residual divergences we have found in the Littlest Higgs model. In this model the scalar partner masses cannot be larger than the cutoff of the theory $\Lambda = 4\pi f$. Using this scale, Peris shows that the axial charge of the constituent quark is reduced by 20% in rough agreement with baryon phenomenology.

The value of the charge form factors of dynamically broken generators will depend on the ultraviolet completion of the Little Higgs model. The principal question concerns how the dynamical symmetry breaking is transmitted to the fermions. As a minimum, the

symmetry breaking is reflected through the Yukawa couplings of the Goldstone bosons to the fermions. In this case the next-to-leading corrections may be estimated from Goldstone loop corrections to the charge form factors and the scale of the logarithmic divergences should not be larger than Λ. However, the light fermions may have a more complex relation to the fundamental fermions of the ultraviolet completion of the theory and the Little Higgs theory may have to include modifications of the charge form factors even at leading order, as in the case of the baryon where $G_A \neq 1$. We conclude that the residual logarithmic divergences found in Section 4 are a real physical effect, but they also indicate additional sensitivity to the ultraviolet completion of the Little Higgs models not usually included in the phenomenology of these models.

Assuming the minimal case discussed above, we estimate the contributions of the logarithmically divergent terms to the functions X and Y. Removing $1/\varepsilon$ terms from (4.7) and setting $\mu = \Lambda$ we find

$$\Delta X_{div} = \Delta Y_{div} = \frac{x_t}{64} \frac{1}{1 - x_L} \frac{v^2}{f^2} \left[\ln \frac{\Lambda^2}{M_\Phi^2} - \frac{1}{5} \ln \frac{\Lambda^2}{M_{W_L}^2} \right]. \tag{5.1}$$

Setting

$$\Lambda = 4\pi f, \qquad m_H = 115\,\text{GeV}, \qquad v = 246\,\text{GeV} \tag{5.2}$$

and using the values of M_{W_L} and m_t in table 3 we find for $f/v = 5$ and $x_L = 0.8$

$$\Delta X_{div} = \Delta Y_{div} = 0.049, \tag{5.3}$$

which should be compared with $X_{\text{SM}} \simeq 1.49$ and $Y_{\text{SM}} \simeq 0.95$. Thus for this choice of parameters the correction amounts to 3% and 5% for X and Y, respectively. Larger values are obtained for x_L closer to unity but such values are disfavoured by the measured value of ΔM_s as discussed in the next section. Smaller values are found for larger f. In summary the effect of the logarithmic divergences turns out to be small. However, we would like to emphasize that our estimate takes only into account the contributions, where the fermions only couple to the Goldstone bosons through the mass terms, not the G_A-like terms, and the sensitivity to the ultraviolet completion of the LH model could in principle be larger than estimated here.

Few technical details on the issue of divergences are given in Appendix C.

6. Implications for Rare K and B Decays

The most recent compendium of formulae for rare decays considered here, in terms of the functions X and Y can be found in two papers on rare decays in a model with one universal extra dimension [34, 35]. In order to obtain the relevant branching ratios in the LH model one only has to replace $X(x_t, 1/R)$ and $Y(x_t, 1/R)$ given there by $X_{\text{LH}}(v)$ and $Y_{\text{LH}}(v)$ calculated here. Moreover, we included the recently calculated NNLO QCD corrections [32] and long distance contributions [33] to $K^+ \to \pi^+ \nu\bar\nu$ that imply $P_c = 0.42 \pm 0.05$ for the charm contribution to this decay.

$\overline{m}_{\mathrm{t}} = 163.8(32)\,\mathrm{GeV}$	$|V_{ub}| = 0.00423(35)$
$M_{\mathrm{W}} = 80.425(38)\,\mathrm{GeV}$	$|V_{cb}| = 0.0416(7)$ [39]
$\alpha = 1/127.9$	$\lambda = 0.225(1)$ [40]
$\sin^2\theta_W = 0.23120(15)$	$\gamma = 71° \pm 16°$ [41]

Table 3: Values of the experimental and theoretical quantities used as input parameters.

As we are mainly interested in the effects of the corrections coming from LH contributions we will consider the ratios

$$R_+ \;\equiv\; \frac{Br\left(K^+ \to \pi^+\nu\bar\nu\right)_{\mathrm{LH}}}{Br\left(K^+ \to \pi^+\nu\bar\nu\right)_{\mathrm{SM}}}, \tag{6.1}$$

$$R_L \;\equiv\; \frac{Br\left(K_L \to \pi^0\nu\bar\nu\right)_{\mathrm{LH}}}{Br\left(K_L \to \pi^0\nu\bar\nu\right)_{\mathrm{SM}}} = \frac{Br\left(B \to X_{s,d}\nu\bar\nu\right)_{\mathrm{LH}}}{Br\left(B \to X_{s,d}\nu\bar\nu\right)_{\mathrm{SM}}} = \left[\frac{X_{\mathrm{LH}}}{X_{\mathrm{SM}}}\right]^2, \tag{6.2}$$

$$R_{s,d} \;\equiv\; \frac{Br\left(B_{s,d} \to \mu^+\mu^-\right)_{\mathrm{LH}}}{Br\left(B_{s,d} \to \mu^+\mu^-\right)_{\mathrm{SM}}} = \left[\frac{Y_{\mathrm{LH}}}{Y_{\mathrm{SM}}}\right]^2, \tag{6.3}$$

where with the values of m_t and M_{W_L} in table 3 we have

$$X_{\mathrm{SM}} = 1.49, \qquad Y_{\mathrm{SM}} = 0.95. \tag{6.4}$$

In writing (6.2) and (6.3) we have assumed that the values of the CKM parameters are the same in the SM and the LH model. As both models belong to the class of MFV models for which the so-called universal unitarity triangle exists [30], this assumption can certainly be justified. Moreover, in principle CKM parameters can be determined from tree level processes independently of new physics contributions. This approach differs from the one followed in [14] where the CKM parameters were determined using $B_d^0 - \bar B_d^0$ mixing. As the relevant one-loop function S_{LH} in the LH model differs from the S_{SM}, the CKM parameters turned out to be different in both models in particular for x_L close to unity. However, for x_L close to unity $(\Delta M_s)_{\mathrm{LH}}$ is significantly larger than $(\Delta M_s)_{\mathrm{SM}}$ in contradiction with the recent CDF data that indicate ΔM_s to be smaller than $(\Delta M_s)_{\mathrm{SM}}$. The large non-perturbative uncertainties in the evaluation of ΔM_s and also ΔM_d do not allow for a derivation of an upper bound on x_L from $B_{d,s}^0 - \bar B_{d,s}^0$ mixings but clearly x_L cannot be as high as the 0.95 used in [14, 18]. Therefore we will choose $x_L \leq 0.8$ in what follows. Moreover, as stated above we will take the CKM parameters to be the same for the SM and LH model and fixed to the central values collected in table 3, where $\overline{m}_{\mathrm{t}} = \overline{m}_{\mathrm{t}}(m_t)$ in the $\overline{\mathrm{MS}}$ scheme. Then the ratios in (6.2) and (6.3) only depend on the one-loop functions X and Y and the dependence on the CKM parameters is only present in (6.1) due to the relevant charm contribution in $K^+ \to \pi^+\nu\bar\nu$ in which the new physics contributions are negligible.

For the three new parameters f, x_L and s (see Section 2 for their definitions) we will choose the ranges

$$f/v = 5 \text{ or } 10, \quad 0.2 \leq x_L \leq 0.80, \quad 0.3 \leq s \leq 0.95. \tag{6.5}$$

This parameter space is larger than the one allowed by other processes [7]-[13] which typically imply $f/v \geq 10$ or even higher. But we want to demonstrate that even for f/v as low as 5, the corrections from LH contributions to X and Y are small.

In figure 7 we show the ratios (6.1)–(6.3) as functions of s for different values of x_L and $f/v = 5$. The corresponding plots for $f/v = 10$ are shown in Fig. 8.

We observe that R_+, R_L and $R_{d,s}$ increase with increasing s and x_L. For $f/v = 5$, $s = 0.95$ and $x_L = 0.8$ they reach 1.23, 1.33 and 1.51, respectively. However for $f/v = 10$ they are all below 1.15 and consequently it will be difficult to distinguish the LH predictions for the branching ratios in question from the SM ones.

7. $B \to X_s\gamma$ Decay

One of the most popular decays used to constrain new physics contributions is the $B \to X_s\gamma$ decay for which the measured branching ratio [39]

$$Br(B \to X_s\gamma)_{\text{exp}} = (3.52 \pm 0.30) \cdot 10^{-4} \tag{7.1}$$

agrees well with the SM NLO prediction [42, 43]

$$Br(B \to X_s\gamma)_{\text{SM}} = (3.33 \pm 0.29) \cdot 10^{-4}, \tag{7.2}$$

both given for $E_\gamma > 1.6\,\text{GeV}$ and the SM prediction for $m_c(m_c)/m_b^{1S} = 0.26$. $Br(B \to X_d\gamma)$ is in the ballpark of $1.5 \cdot 10^{-5}$.

One should emphasize that within the SM this decay is governed by the already well determined CKM element $|V_{ts}|$ so that dominant uncertainties in (7.2) result from the truncation of the QCD perturbative series and the value of $m_c(\mu)$ that enters the branching ratio first at the NLO level. A very difficult NNLO calculation, presently in progress [43], should reduce the error in (7.2) below 10%.

The effective Hamiltonian relevant for this decay within the SM is given as follows

$$\mathcal{H}_{\text{eff}}^{\text{SM}}(\bar{b} \to \bar{s}\gamma) = -\frac{G_F}{\sqrt{2}}V_{ts}V_{tb}^*\left[\sum_{i=1}^{6}C_i(\mu_b)Q_i + C_{7\gamma}(\mu_b)Q_{7\gamma} + C_{8G}(\mu_b)Q_{8G}\right], \tag{7.3}$$

where Q_i are four-quark operators, $Q_{7\gamma}$ is the magnetic photon penguin operator and Q_{8G} the magnetic gluon penguin operator. The explicit expression for the branching ratio $Br(B \to X_s\gamma)$ resulting from (7.3) is very complicated and we will not present it here. It can be found for instance in [42].

For our purposes it is sufficient to know that in the LO approximation the Wilson coefficients $C_{7\gamma}$ and C_{8G} are given at the renormalization scale $\mu_W = \mathcal{O}(M_W)$ as follows

$$C_{7\gamma}^0(\mu_W) = -\frac{1}{2}D_0'(x_t), \qquad C_{8G}^0(\mu_W) = -\frac{1}{2}E_0'(x_t), \tag{7.4}$$

with the explicit expressions for $D_0'(x_t)$ and $E_0'(x_t)$ given by

$$D_0'(x_t) = \frac{(8x_t^3 + 5x_t^2 - 7x_t)}{12(x_t - 1)^3} - \frac{(3x_t^3 - 2x_t^2)\log x_t}{2(x_t - 1)^4}, \tag{7.5}$$
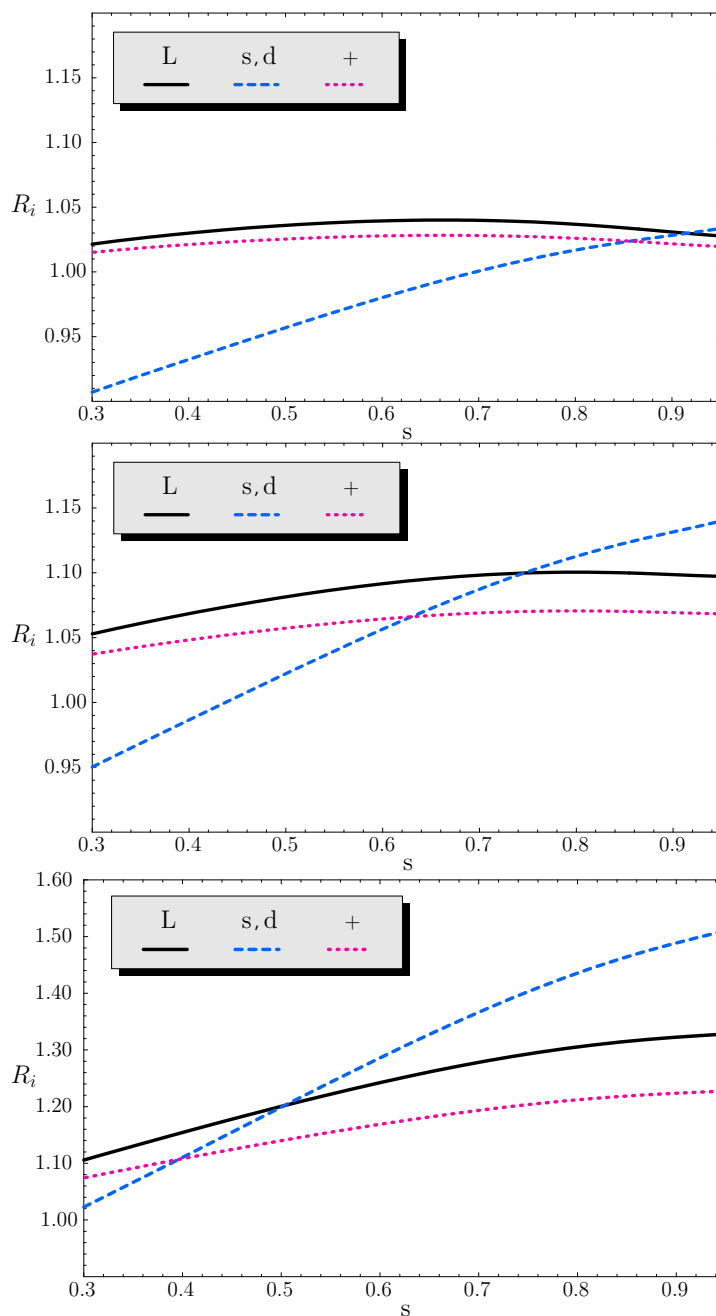
Figure 7: Normalized branching ratios R_L, $R_{s,d}$, R_+ for different $x_L = 0.2, 0.5, 0.8$ (from top to bottom) and $f/v = 5$.

$$E_0'(x_t) = \frac{(x_t^3 - 5x_t^2 - 2x_t)}{4(x_t - 1)^3} + \frac{3x_t^2 \log x_t}{2(x_t - 1)^4}. \tag{7.6}$$

In view of the importance of QCD corrections in this decay we will include these corrections at NLO in the SM part, but only at LO in the new contributions. This amounts
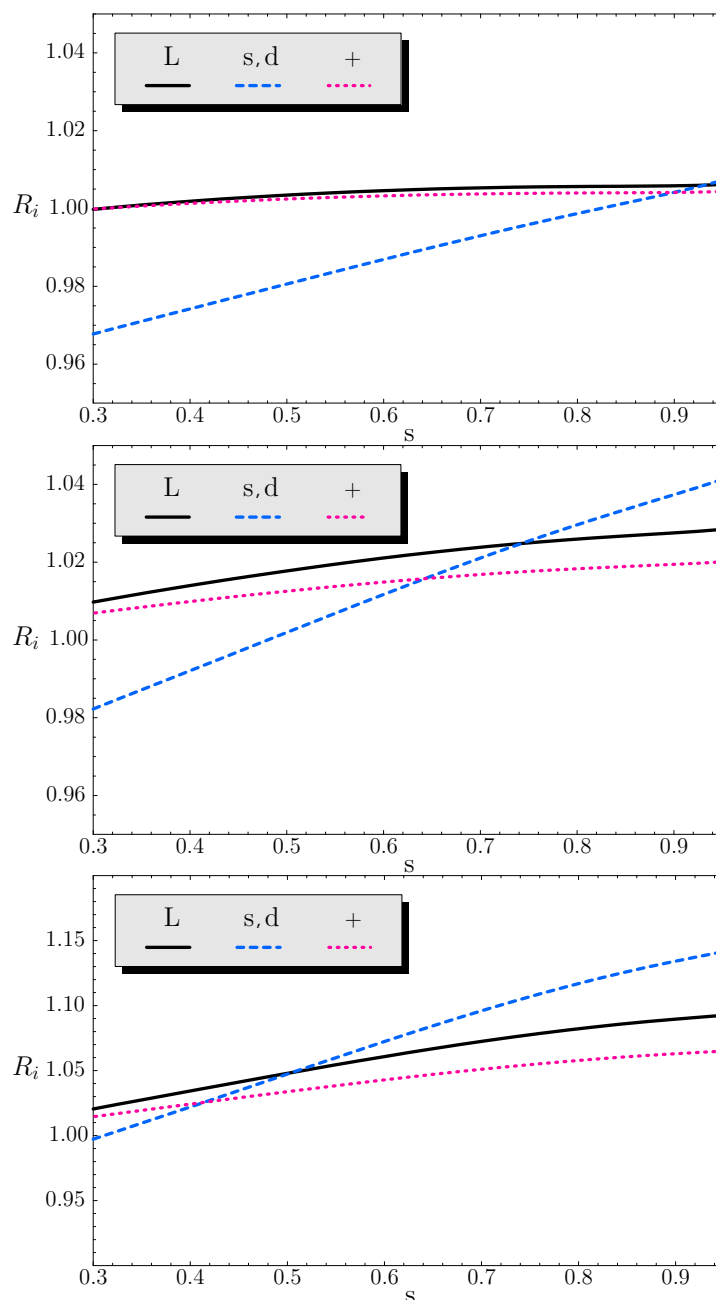
Figure 8: Normalized branching ratios R_L, $R_{s,d}$, R_+ for different $x_L = 0.2, 0.5, 0.8$ (from top to bottom) and $f/v = 10$.

to including only corrections to the renormalization of the operators in the LH part and eventually to increase the scale μ_W to $\mu \approx 500\,\text{GeV}$ at which the new particles are integrated out. As the dominant QCD corrections to $Br(B \to X_s\gamma)$ come anyway from the renormalization group evolution from μ_W down to $\mu_b = \mathcal{O}(m_b)$ and the matrix elements of

the operators Q_2 and $Q_{7\gamma}$ at μ_b, these dominant corrections are common to the SM and LH parts.

Within the LO approximation the new physics contributions to $B \to X_s \gamma$ enter only through the modifications of the functions $D'_0(x_t)$ and $E'_0(x_t)$. This modification can be directly obtained by changing the arguments in $D'_0(x_t)$ and $E'_0(x_t)$ and introducing corresponding factors that distinguish the LH model from SM contribution. It is easy to see that the contributions with internal $(t, W_H^\pm)$ and $(T, W_H^\pm)$ are $\mathcal{O}(v^4/f^4)$, while the contributions involving charged Higgs $\Phi^\pm$ enter first at even higher order. Consequently only the diagrams involving W_L, t and T contribute at $\mathcal{O}(v^2/f^2)$. We find then

$$\left[D'_0(x_t, x_T) \right]_{\text{LH}} = D'_0(x_t) + \Delta D'_0, \qquad \left[E'_0(x_t, x_T) \right]_{\text{LH}} = E'_0(x_t) + \Delta E'_0, \qquad (7.7)$$

where

$$\Delta D'_0 = \frac{v^2}{f^2} \left[x_L^2 (D'_0(x_T) - D'_0(x_t)) - 2a\, D'_0(x_t) \right]. \qquad (7.8)$$

$\Delta E'_0$ is obtained from this equation by simply replacing D'_0 by E'_0.

The first calculation of $B \to X_s \gamma$ decay within the LH model has been presented in [23] and the result given above confirms the one quoted in that paper.

As in [23] we find that the LH corrections amount to at most 3% and are consequently smaller than the experimental and theoretical uncertainties in (7.1) and (7.2).

8. Conclusions

In this paper we have presented for the first time a complete analysis of $\mathcal{O}(v^2/f^2)$ contributions to rare K and B decays in the LH model of [1]-[5]. The resulting corrections turned out to be small for values of the high energy scale $f = \mathcal{O}(2-3)\,\text{TeV}$ as required by electroweak precision studies. While this is at first sight disappointing, one should recall the upper bounds on rare decay branching ratios in MFV models [44] that do not allow for large departures from the SM predictions within the MFV scenario. Thus the LH model considered here is consistent with these bounds.

On the technical side we have given a complete list of Feynman rules relevant for the calculation of penguin and box diagrams that could be used for other processes. As a byproduct we have also presented for the first time the calculations of the X and Y functions in the unitary gauge both in the SM and the LH model. Some of the results obtained here can be used to calculate the T–even contributions to rare decays in the LH model with T–parity [38].

Probably the most interesting result of our paper is the left-over singularity that signals some sensitivity of the final result to the UV completion of the theory. A detailed discussion of this issue and of possible implications of these findings for other LH models can be found in Section 5. A similar singularity has been found independently in the context of the study of electroweak precision constraints in [45].

Large new physics effects have been found recently in the case of $B_{d,s}^0 - \bar{B}_{d,s}^0$ mixing in the LH model with T-parity, where the presence of mirror fermions implies non-MFV interactions [37, 46]. The analysis of rare K and B decays presented here will be generalized to this model in [38].

Acknowledgments

A. The Fermion Sector

In order to calculate $\mathcal{O}(v^4/f^4 x_T)$ terms in classes 4 and 5 we had to generalize the rules of [7] by including certain higher order terms in v/f. Here we present some details of this derivation that also summarize the differences between our work and [7] discussed in detail in [14].

The Yukawa Lagrangian for the top sector is given by [7]

$$\mathcal{L}_t = \lambda_2 f \tilde{t} \tilde{t}'^c - i\lambda_1 t_3 \left[\sqrt{2} h^0 + \frac{i}{f}(h^- \phi^+ + \sqrt{2} h^{0*} \phi^0) \right] u_3'^c$$
$$+ i\lambda_1 \tilde{t} \left[-if + \frac{i}{f}(h^+ h^- + h^0 h^{0*} + 2\phi^{++}\phi^{--} + 2\phi^+ \phi^- + 2\phi^0 \phi^{0*}) \right] u_3'^c + h.c. \quad \text{(A.1)}$$

where t_3 and $\tilde{t}$ are two components of the left handed vector like fields $\chi_i = (b_3, t_3, \tilde{t})$ replacing the third SM quark doublet and $u_3'^c$ and $\tilde{t}'^c$ are the corresponding right handed singlets. h and ϕ are the doublet and triplet scalar fields of the unbroken $SU(2)_L \otimes U(1)_Y$. Spontaneous symmetry breaking via the vacuum expectation values of the h and ϕ fields, $\langle h^0 \rangle = v/\sqrt{2}$ and $\langle i\phi^0 \rangle = v'$ generates the fermion masses. In the following we set $v' = 0$ as we did in our analysis. Diagonalizing the Lagrangian (A.1), one obtains the left and right handed mass eigenstates of the light and the heavy top quark. The field rotation, that has to be performed, is given by

$$t_L = c_L t_3 - s_L \tilde{t}, \qquad\qquad t_R^c = c_R u_3'^c - s_R \tilde{t}'^c, \qquad\qquad \text{(A.2)}$$
$$T_L = c_L t_3 + s_L \tilde{t}, \qquad\qquad T_R^c = c_R u_3'^c + s_R \tilde{t}'^c, \qquad\qquad \text{(A.3)}$$

where we find

$$s_R = \frac{\lambda_1}{\sqrt{\lambda_1^2 + \lambda_2^2}} \left(1 - \frac{v^2}{f^2} \frac{\lambda_2^2}{\lambda_1^2 + \lambda_2^2} \left(\frac{1}{2} - \frac{\lambda_1^2}{\lambda_1^2 + \lambda_2^2} \right) + \mathcal{O}(v^4/f^4) \right), \qquad \text{(A.4)}$$

$$c_R = \frac{\lambda_2}{\sqrt{\lambda_1^2 + \lambda_2^2}} \left(1 + \frac{v^2}{f^2} \frac{\lambda_1^2}{\lambda_1^2 + \lambda_2^2} \left(\frac{1}{2} - \frac{\lambda_1^2}{\lambda_1^2 + \lambda_2^2} \right) + \mathcal{O}(v^4/f^4) \right), \qquad \text{(A.5)}$$

$$s_L = \frac{\lambda_1^2}{\lambda_1^2 + \lambda_2^2} \frac{v}{f} \left(1 + \frac{v^2}{f^2} \left(-\frac{5}{6} + \frac{1}{2} \frac{\lambda_1^4}{(\lambda_1^2 + \lambda_2^2)^2} + 2 \frac{\lambda_1^2}{\lambda_1^2 + \lambda_2^2} \left(1 - \frac{\lambda_1^2}{\lambda_1^2 + \lambda_2^2} \right) \right) \right)$$
$$+ \mathcal{O}(v^4/f^4), \qquad\qquad\qquad\qquad\qquad \text{(A.6)}$$

$$c_L = 1 - \frac{v^2}{f^2} \frac{1}{2} \frac{\lambda_1^4}{(\lambda_1^2 + \lambda_2^2)^2} + \mathcal{O}(v^4/f^4). \tag{A.7}$$

In order to obtain positive and real valued masses, it is necessary to absorb a factor $-i$ into the t_3 field in (A.1). A field redefinition of this kind was suggested but not performed by the authors of [7]. Then the masses of the light and the heavy top quark are given by

$$m_t = \frac{v\lambda_1\lambda_2}{\sqrt{\lambda_1^2 + \lambda_2^2}} \left(1 + \frac{v^2}{f^2} \left(-\frac{1}{3} + \frac{1}{2} \frac{\lambda_1^2}{\lambda_1^2 + \lambda_2^2} \left(1 - \frac{\lambda_1^2}{\lambda_1^2 + \lambda_2^2} \right) \right) + \mathcal{O}(v^4/f^4) \right), \tag{A.8}$$

$$m_T = f\sqrt{\lambda_1^2 + \lambda_2^2} \left(1 - \frac{v^2}{f^2} \frac{1}{2} \frac{\lambda_1^2}{\lambda_1^2 + \lambda_2^2} \left(1 - \frac{\lambda_1^2}{\lambda_1^2 + \lambda_2^2} \right) + \mathcal{O}(v^4/f^4) \right). \tag{A.9}$$

The formulae of this section differ from the ones in [7] in the following points:

- The masses m_t and m_T in (A.8) and (A.9) are real valued and positive.

- s_R and c_R have the opposite sign in front of the last term of the $\mathcal{O}(v^2/f^2)$ expressions.

B. Tables of Singularities

C. Comments on the Leftover Singularities

In Section 5 we found that in the amplitudes for FCNCs leftover singularities remained. As pointed out these divergent terms do not depend on the choice of a special gauge. This led to the conclusion that these divergences are a real physical effect and can be identified as a renormalization of the quark charges. In our calculation the divergent quark vertex contribution, using fundamental gauge fields, reads

$$V_{quark} = \frac{1}{4} (\lambda_1 v)^2 \frac{1}{(4\pi)^2} \frac{1}{\varepsilon} \tilde{V}_{quark} \gamma_\mu (1 - \gamma_5), \tag{C.1}$$

where $\tilde{V}_{quark}$ is given by

$$\tilde{V}_{quark} = \frac{4}{v^2} \left\{ \frac{1}{4} \left(g_1 W_1^3 \right) - \frac{1}{4} \left(g_2 W_2^3 \right) + \frac{1}{20} \left(g_1' B_1 \right) - \frac{1}{20} \left(g_2' B_2 \right) \right\}. \tag{C.2}$$

Rewriting this result in a mass diagonal basis then yields

$$\tilde{V}_{quark} = \frac{1}{v^2} \frac{g}{sc} Z_H + \frac{1}{5} \frac{1}{v^2} \frac{g'}{s'c'} A_H + \frac{1}{2} \frac{1}{f^2} \left[-c^2 + s^2 + c'^2 - s'^2 \right] \sqrt{g^2 + g'^2} Z_L. \tag{C.3}$$

As it can be seen from (C.3) the coefficient of the physical Z-boson is suppressed in two different scenarios:

- if the gauge couplings of the two gauge groups are identical, i.e. $c = s$ and $c' = s'$. This, for example, happens in the case of the T-even sector of the Littlest Higgs Model with T-parity [38], where c and s are set to $c = s = 1/\sqrt{2} = c' = s'$.

- if one of the product gauge groups is strongly coupled, i.e. if $c, c' \approx 1$ or $s, s' \approx 1$.

	Column 1	Column 2	Column 3	Column 4
Class 1.	Diagrams shown in figure 1.			
1	$\frac{x_t}{\varepsilon}\left(-\frac{1}{16}+\frac{v^2}{f^2}\left(\frac{5}{8}a-\frac{1}{8}u+\frac{5}{8}a'+\frac{1}{16}ux_L\right)\right)$			$\frac{x_t}{\varepsilon}\left(\frac{1}{16}+\frac{v^2}{f^2}\left(-\frac{1}{4}a\right)\right)$
2	$\frac{x_t}{\varepsilon}\frac{v^2}{f^2}\left(-\frac{3}{8}a\right)$	$\frac{x_t}{\varepsilon}\frac{v^2}{f^2}\left(\left(c'^2-\frac{2}{5}\right)^2\left(-\frac{5}{16}\right)-\frac{1}{8}x_L\left(c'^2-\frac{2}{5}\right)\right)$		
	Custodial Correction: $\frac{x_t}{\varepsilon}\frac{v^2}{f^2}\left(-\frac{5}{64}(c'^2-s'^2)^2\right)$			
Class 2.	Diagrams shown in figure 2.			
1	$\frac{x_t}{\varepsilon}\frac{v^2}{f^2}\left(-\frac{1}{4}c^4\right)\left(1-s_w^2\right)$	$\frac{x_t}{\varepsilon}\frac{v^2}{f^2}\left(\frac{3}{8}c^4\right)\left(1-s_w^2\right)$	$\frac{x_t}{\varepsilon}\frac{v^2}{f^2}\left(-\frac{3}{16}c^4\right)\left(1-\frac{2}{3}s_w^2\right)$	$\frac{x_t}{\varepsilon}\frac{v^2}{f^2}\left(\frac{1}{8}c^4\right)$
2	$\frac{x_t}{\varepsilon}\frac{v^2}{f^2}\left(-\frac{1}{4}c^4\right)$	$\frac{x_t}{\varepsilon}\frac{v^2}{f^2}\left(-\frac{3}{16}c^4\right)$	$\frac{x_t}{\varepsilon}\frac{v^2}{f^2}\left(+\frac{3}{8}c^4\right)$	
Class 3.	Diagrams shown in figure 3.			
1	$\frac{x_t}{\varepsilon}\frac{v^2}{f^2}x_L^2\left(\frac{1}{2}-\frac{1}{4}s_w^2\right)$	$\frac{x_t}{\varepsilon}\frac{v^2}{f^2}x_L^2\left(-\frac{3}{8}\right)\left(1-s_w^2\right)$	$\frac{x_t}{\varepsilon}\frac{v^2}{f^2}x_L^2\left(\frac{3}{16}-\frac{1}{8}s_w^2\right)$	
2	$\frac{x_t}{\varepsilon}\frac{v^2}{f^2}x_L^2\left(-\frac{1}{16}\right)$	$\frac{x_T}{\varepsilon}\frac{v^2}{f^2}x_L^2\left(\frac{1}{4}s_w^2\right)$	$\frac{x_T}{\varepsilon}\frac{v^2}{f^2}x_L^2\left(\frac{3}{8}\right)\left(1-s_w^2\right)$	
3	$\frac{x_T}{\varepsilon}\frac{v^2}{f^2}x_L^2\left(-\frac{3}{16}+\frac{1}{8}s_w^2\right)$	$\left(\frac{x_t}{\varepsilon}+\frac{x_T}{\varepsilon}\right)\frac{v^2}{f^2}x_L^2\left(-\frac{1}{4}\right)$	$\frac{x_T}{\varepsilon}\frac{v^2}{f^2}x_L^2\left(\frac{1}{16}\right)$	

Table 4: $1/\varepsilon$ Singularities to $\mathcal{O}(v^2/f^2)$ of the Classes 1-3. The entries are arranged according to the position of the corresponding diagrams in figure 1–3.

References

[1] N. Arkani-Hamed, A.G. Cohen and H. Georgi, *Electroweak symmetry breaking from dimensional deconstruction*, *Phys. Lett.* **B 513** (2001) 232 [hep-ph/0105239].

[2] N. Arkani-Hamed, A.G. Cohen, T. Gregoire and J.G. Wacker, *Phenomenology of electroweak symmetry breaking from theory space*, *JHEP* **08** (2002) 020 [hep-ph/0202089].

[3] N. Arkani-Hamed et al., *The minimal moose for a little Higgs*, *JHEP* **08** (2002) 021 [hep-ph/0206020].

[4] N. Arkani-Hamed, A.G. Cohen, E. Katz and A.E. Nelson, *The littlest Higgs*, *JHEP* **07** (2002) 034 [hep-ph/0206021].

	Column 1	Column 2	Column 3	Column 4
Class 4.	Diagrams shown in figure 4.			
1	$\frac{x_T}{\varepsilon}\frac{v^2}{f^2}\frac{c^2}{s^2}x_L^2\frac{1}{y}\left(-\frac{1}{4}\right)$	$\frac{x_T}{\varepsilon}\frac{v^2}{f^2}\frac{c^2}{s^2}x_L^2\frac{1}{y}\left(\frac{3}{8}\right)$	$\frac{x_T}{\varepsilon}\frac{v^2}{f^2}\frac{c^2}{s^2}x_L^2\frac{1}{y}\left(-\frac{3}{16}\right)$	$\frac{x_T}{\varepsilon}\frac{v^2}{f^2}\frac{c^2}{s^2}x_L^2\frac{1}{y}\left(\frac{1}{8}\right)$
2	$\frac{x_T}{\varepsilon}\frac{v^2}{f^2}\frac{c^2}{s^2}x_L^2\frac{1}{y}\left(-\frac{1}{4}\right)$	$\frac{x_T}{\varepsilon}\frac{v^2}{f^2}\frac{c^2}{s^2}x_L^2\frac{1}{y}s_w^2\left(\frac{1}{4}\right)$	$\frac{x_T}{\varepsilon}\frac{v^2}{f^2}\frac{c^2}{s^2}x_L^2\frac{1}{y}(1-s_w^2)\left(\frac{3}{8}\right)$	$\frac{x_T}{\varepsilon}\frac{v^2}{f^2}\frac{c^2}{s^2}x_L^2\frac{1}{y}(\frac{2}{3}s_w^2-1)\left(\frac{3}{16}\right)$
Class 5.	Diagrams shown in figure 5.			
1	$\frac{v^2}{f^2}\frac{x_t}{\varepsilon}\left(-\frac{1}{10}x_L+\frac{1}{4}c'^2x_L\right)$ $+\frac{v^4}{f^4}\frac{x_T}{\varepsilon}x_L^2\left(\frac{1}{2}c'^2-\frac{5}{4}c'^4\right)$	$\frac{v^4}{f^4}\frac{x_T}{\varepsilon}x_L^2\left(\frac{1}{20}-\frac{5}{8}c'^2+\right.$ $\left.+\frac{5}{4}c'^4-\frac{1}{20}x_L+\frac{1}{8}c'^2x_L\right)$	$\frac{v^4}{f^4}\frac{x_T}{\varepsilon}x_L^2\left(-\frac{1}{20}+\right.$ $\left.+\frac{1}{4}c'^2-\frac{5}{16}c'^4\right)$	
2	$\frac{v^4}{f^4}\frac{x_T}{\varepsilon}x_L^2\left(-\frac{3}{8}a\right)$	$\frac{v^4}{f^4}\frac{x_T}{\varepsilon}x_L^2\left(1-s_w^2\right)$ $\left(-\frac{9}{8}a+\frac{3}{4}d_2+\frac{3}{8}u-\frac{15}{8}a'\right)$	$\frac{v^4}{f^4}\frac{x_T}{\varepsilon}x_L^2\left(\frac{1}{16}u-\frac{1}{16}ux_L-\frac{5}{4}a'-\frac{1}{4}x_L^2\right.$ $\left.+s_w^2\left(-\frac{3}{4}a+\frac{1}{2}d_2+\frac{1}{4}u-\frac{5}{4}a'\right)\right)$	
3	$\frac{v^2}{f^2}\frac{x_t}{\varepsilon}x_L\left(-\frac{1}{8}u\right)+\frac{v^4}{f^4}\frac{x_T}{\varepsilon}x_L^2$ $\left(a-\frac{1}{2}d_2-\frac{1}{4}u+\frac{1}{4}x_L^2+\frac{5}{2}a'\right)$	$\frac{v^4}{f^4}\frac{x_T}{\varepsilon}x_L^2\left(\frac{3}{4}a-\frac{3}{8}d_2-\frac{1}{4}u+\frac{5}{4}a'+\right.$ $\left.s_w^2\left(-\frac{3}{8}a+\frac{1}{4}d_2+\frac{1}{8}u-\frac{5}{8}a'\right)\right)$	$\frac{v^4}{f^4}\frac{x_T}{\varepsilon}x_L^2\left(-\frac{1}{4}a+\frac{1}{8}d_2\right)$	
	Custodial Correction: $\frac{x_T}{\varepsilon}\frac{v^4}{f^4}x_L^2\left(-\frac{5}{64}(c'^2-s'^2)^2\right)$			

Table 5: $1/\varepsilon$ Singularities to $\mathcal{O}(v^2/f^2)$ of the Classes 4 and 5. The entries are arranged according to the position of the corresponding diagrams in figure 4 and 5.

Class 6.	Diagrams shown in figure 6.		
Line	Column 1	Column 2	Column 3
1	$\frac{x_t}{\varepsilon}\frac{v^2}{f^2}\left(-\frac{1}{48}s_w^2\right)$	$\frac{x_t}{\varepsilon}\frac{v^2}{f^2}\left(\frac{1}{32}s_w^2\right)$	$\frac{x_t}{\varepsilon}\frac{v^2}{f^2}\left(\frac{1}{64}\right)\left(1-\frac{2}{3}s_w^2\right)$
2	$\frac{x_t}{\varepsilon}\frac{v^2}{f^2}\left(-\frac{1}{48}s_w^2\right)\frac{x_L}{1-x_L}$	$\frac{x_t}{\varepsilon}\frac{v^2}{f^2}\left(\frac{1}{32}s_w^2\right)\frac{x_L}{1-x_L}$	$\frac{x_t}{\varepsilon}\frac{v^2}{f^2}\left(\frac{1}{64}\right)\left(1-\frac{2}{3}s_w^2\right)\frac{x_L}{1-x_L}$

Table 6: $1/\varepsilon$ Singularities to $\mathcal{O}(v^2/f^2)$ in Class 6 The entries are arranged according to the position of the corresponding diagrams in figure 6.

[5] I. Low, W. Skiba and D. Smith, *Little Higgses from an antisymmetric condensate*, *Phys. Rev.* **D 66** (2002) 072001 [hep-ph/0207243].

[6] M. Schmaltz and D. Tucker-Smith, *Little Higgs review*, *Ann. Rev. Nucl. Part. Sci.* **55** (2005)

229–270 [hep-ph/0502182];

M. Perelstein, *Little Higgs models and their phenomenology*, hep-ph/0512128.

[7] T. Han, H.E. Logan, B. McElrath and L.-T. Wang, *Phenomenology of the little Higgs model*, *Phys. Rev.* **D 67** (2003) 095004 [hep-ph/0301040].

[8] C. Csáki, J. Hubisz, G.D. Kribs, P. Meade and J. Terning, *Big corrections from a little Higgs*, *Phys. Rev.* **D 67** (2003) 115002 [hep-ph/0211124].

[9] J.L. Hewett, F.J. Petriello and T.G. Rizzo, *Constraining the littlest Higgs*, *JHEP* **10** (2003) 062 [hep-ph/0211218].

[10] M.-C. Chen and S. Dawson, *One-loop radiative corrections to the rho parameter in the littlest Higgs model*, *Phys. Rev.* **D 70** (2004) 015003 [hep-ph/0311032]; *The littlest Higgs model and one-loop electroweak precision constraints*, hep-ph/0409163.

[11] C.X. Yue and W. Wang, *The branching ratio r(b) in the littlest Higgs model*, *Nucl. Phys.* **B 683** (2004) 48 [hep-ph/0401214].

[12] W. Kilian and J. Reuter, *The low-energy structure of little Higgs models*, *Phys. Rev.* **D 70** (2004) 015004 [hep-ph/0311095].

[13] T. Han, H.E. Logan, B. McElrath and L.-T. Wang, *Loop induced decays of the little Higgs: $H \to gg, \gamma\gamma$*, *Phys. Lett.* **B 563** (2003) 191 [hep-ph/0302188].

[14] A.J. Buras, A. Poschenrieder and S. Uhlig, *Particle antiparticle mixing, ϵ_k and the unitarity triangle in the littlest Higgs model*, *Nucl. Phys.* **B 716** (2005) 173 [hep-ph/0410309].

[15] S.R. Choudhury, N. Gaur, A. Goyal and N. Mahajan, *$B_d - \bar{B}_d$ mass difference in little Higgs model*, *Phys. Lett.* **B 601** (2004) 164 [hep-ph/0407050].

[16] J.Y. Lee, *A vector-like heavy quark in the littlest Higgs model*, *JHEP* **12** (2004) 065 [hep-ph/0408362].

[17] S. Fajfer and S. Prelovsek, *Effects of littlest Higgs model in rare D meson decays*, *Phys. Rev.* **D 73** (2006) 054026 [hep-ph/0511048].

[18] A.J. Buras, A. Poschenrieder and S. Uhlig, *Non-decoupling effects of the heavy T in the $B^0_{d,s} - \bar{B}^0_{d,s}$ mixing and rare K and B decays*, hep-ph/0501230.

[19] CDF - Run II collaboration, *Measurement of the B^0_s-$\bar{B}^0_s$ oscillation frequency*, *Phys. Rev. Lett.* **97** (2006) 062003 [hep-ex/0606027].

[20] D0 collaboration, V.M. Abazov et al., *First direct two-sided bound on the B^0_s oscillation frequency*, *Phys. Rev. Lett.* **97** (2006) 021802 [hep-ex/0603029].

[21] M. Blanke, A.J. Buras, D. Guadagnoli and C. Tarantino, *Minimal flavour violation waiting for precise measurements of ΔM_s, $|V(ub)|$, γ and $B^0_{s,d} \to \mu^+\mu^-$*, *JHEP* **10** (2006) 003 [hep-ph/0604057].

[22] P. Ball and R. Fleischer, *Probing new physics through b mixing: status, benchmarks and prospects*, hep-ph/0604249.

[23] W.-J. Huo and S.-H. Zhu, *$B \to s\gamma$ in littlest Higgs model*, *Phys. Rev.* **D 68** (2003) 097301 [hep-ph/0306029].

[24] S.R. Choudhury, N. Gaur, G.C. Joshi and B.H.J. McKellar, *$K_L \to \pi^0 \nu\bar{\nu}$ in little Higgs model*, hep-ph/0408125.

[25] S.L. Glashow, J. Iliopoulos and L. Maiani, *Weak interactions with lepton-hadron symmetry*, *Phys. Rev.* **D 2** (1970) 1285.

[26] S. Peris, G_a *in the constituent quark model*, *Phys. Lett.* **B 268** (1991) 415.

[27] For the most recent reviews see A.J. Buras, F. Schwab and S. Uhlig, *Waiting for precise measurements of $K^+ \to \pi^+ \nu\bar{\nu}$ and $K_L \to \pi^0 \nu\bar{\nu}$*, `hep-ph/0405132`;
G. Isidori, *Flavor physics with light quarks and leptons*, *ECONF* **C060409** (2006) 035 [`hep-ph/0606047`].

[28] T. Inami and C.S. Lim, *Effects of superheavy quarks and leptons in low-energy weak processes $K_L \to \mu\bar{\mu}$, $K^+ \to \pi^+ \nu\bar{\nu}$ and $K^0 \to \bar{K}^0$*, *Prog. Theor. Phys.* **65** (1981) 297.

[29] G. Buchalla, A.J. Buras and M.K. Harlander, *Penguin box expansion: flavor changing neutral current processes and a heavy top quark*, *Nucl. Phys.* **B 349** (1991) 1.

[30] A.J. Buras, P. Gambino, M. Gorbahn, S. Jager and L. Silvestrini, *Universal unitarity triangle and physics beyond the standard model*, *Phys. Lett.* **B 500** (2001) 161 [`hep-ph/0007085`];
G. D'Ambrosio, G.F. Giudice, G. Isidori and A. Strumia, *Minimal flavour violation: an effective field theory approach*, *Nucl. Phys.* **B 645** (2002) 155 [`hep-ph/0207036`];
A.J. Buras, *Minimal flavor violation*, *Acta Phys. Polon.* **B34** (2003) 5615 [`hep-ph/0310208`].

[31] G. Buchalla, A.J. Buras and M.E. Lautenbacher, *Weak decays beyond leading logarithms*, *Rev. Mod. Phys.* **68** (1996) 1125 [`hep-ph/9512380`].

[32] A.J. Buras, M. Gorbahn, U. Haisch and U. Nierste, *The rare decay $K^+ \to \pi^+ \nu\bar{\nu}$ at the next-to-next- to-leading order in QCD*, `hep-ph/0508165`; *Charm quark contribution to $K^+ \to \pi^+ \nu\bar{\nu}$ at next-to-next-to-leading order*, `hep-ph/0603079`.

[33] G. Isidori, F. Mescia and C. Smith, *Light-quark loops in $K \to \pi\nu\nu$*, *Nucl. Phys.* **B 718** (2005) 319 [`hep-ph/0503107`].

[34] A.J. Buras, M. Spranger and A. Weiler, *The impact of universal extra dimensions on the unitarity triangle and rare K and B decays*, *Nucl. Phys.* **B 660** (2003) 225 [`hep-ph/0212143`].

[35] A.J. Buras, A. Poschenrieder, M. Spranger and A. Weiler, *The impact of universal extra dimensions on $B \to X_s\gamma$, $B \to X_s gluon$, $B \to X_s\mu^+\mu^-$, $K_L \to \pi^0 e^+ e^-$ and ϵ'/ϵ*, *Nucl. Phys.* **B 678** (2004) 455 [`hep-ph/0306158`].

[36] J. Hubisz and P. Meade, *Phenomenology of the littlest Higgs with T-parity*, *Phys. Rev.* **D 71** (2005) 035016 [`hep-ph/0411264`].

[37] J. Hubisz, S.J. Lee and G. Paz, *The flavor of a little Higgs with T-parity*, *JHEP* **06** (2006) 041 [`hep-ph/0512169`].

[38] M. Blanke, A. J. Buras, A. Poschenrieder, S. Recksiegel, C. Tarantino, S. Uhlig and A. Weiler, *Rare and CP-violating K and B decays in the littlest Higgs model with T-parity*, `hep-ph/0610298`.

[39] The Heavy Flavour Averaging Group (HFAG), `http://www.slac.stanford.edu/xorg/hfag/`.

[40] E. Blucher et al., *Status of the Cabibbo angle (CKM2005 - WG 1)*, `hep-ph/0512039`.

[41] UTFIT collaboration, M. Bona et al., *The UTfit collaboration report on the status of the unitarity triangle beyond the standard model, I. Model-independent analysis and minimal flavour violation*, *JHEP* **03** (2006) 080 [`hep-ph/0509219`]; *The UTfit collaboration report on the unitarity triangle beyond the standard model: spring 2006*, `http://utfit.roma1.infn.it` `hep-ph/0605213`.

[42] P. Gambino and M. Misiak, *Quark mass effects in $\bar{B} \to X_s \gamma$*, *Nucl. Phys.* **B 611** (2001) 338 [hep-ph/0104034].

[43] M. Misiak et al., *The first estimate of $B(\bar{B} \to X_s \gamma)$ at $O(\alpha_s^2)$*, hep-ph/0609232.

[44] C. Bobeth et al., *Upper bounds on rare K and B decays from minimal flavor violation*, *Nucl. Phys.* **B 726** (2005) 252 [hep-ph/0505110].

[45] H.-C. Cheng and I. Low, *Little hierarchy, little higgses and a little symmetry*, *JHEP* **08** (2004) 061 [hep-ph/0405243].

[46] M. Blanke et al., *Particle antiparticle mixing, ϵ_k, $\Delta\Gamma_q$, A_{SL}^q, $A_{\rm CP}(B_d \to \psi K_S)$, $A_{\rm CP}(B_s \to \psi\phi)$, and $B \to X_{s,d}\gamma$ in the littlest Higgs model with T-parity*, hep-ph/0605214.